2009

Characterization of electrowetting systems for microfluidic applications

Pradeep K. Mishra
University of South Florida

Characterization of Electrowetting Systems for Microfluidic Applications

by

Pradeep K. Mishra

A thesis submitted in partial fulfillment
of the requirements for the degree of
Master of Science in Mechanical Engineering
Department of Mechanical Engineering
College of Engineering
University of South Florida

Major Professor: Nathan B. Crane, Ph.D.
Alex Volinsky, Ph.D.
Craig Lusk, Ph.D.

Date of Approval:
July 1, 2009

Keywords: Contact Angle, Corrosion, Impedance, Reliability, CYTOP™

DEDICATION

To my Parents

ACKNOWLEDGEMENTS

The author wishes to acknowledge the gracious support of the many people that contributed to this work directly or indirectly. First of all, I am grateful to Prof. Nathan B. Crane for giving me the opportunity to undertake this work. He has been an advisor to me in more ways than just academically. He has been a great source of inspirations during course of this research work.

The time and effort of Dr. Criag Lusk and Dr. Alex Volinsky as committee members are greatly appreciated. The permission to use X-ray diffraction lab (Dr. Alex Volinsky) and Corrosion lab (Dr. Alberto Sagues) for various experimental works is greatly appreciated.

I am greatly thankful to all my colleagues at research lab for their help and support. My special thanks to Vivek Ramadoss for his valuable advices in early days of my graduate studies. My thanks to Mike Nellis, Jeffrey L. Murray, Jairo Chimento, James Tuckerman, Ajay Rajgadkar and Gary Handrick for their help and great company. Thanks to Kartikay Singh for giving excellent company outside the lab.

Without my parent's early support and encouragement, I never would have made it this far. My sincere thanks to my brothers and their family for having faith in me.

Most of all I'm certainly indebted to my best friend, Shikha, for her constant support and motivation. She has been amazing in all aspects. Thank you, I owe a lot to you

This work has been supported in part through NACE Seed Grant 2008-09.

TABLE OF CONTENTS

LIST OF TABLES

LIST OF FIGURES

Characterization of Electrowetting Systems for Microfluidic Applications

Pradeep K. Mishra

ABSTRACT

Electrowetting is the change in apparent surface energy in the presence of an electric field. Recently, this phenomenon has been used to control the shape and location of individual droplets on a surface. However, many microfluidics researchers have acknowledged unexplained behaviors and performance degradation. In this work, electrowetting systems are characterized with different methods. The electrowetting response is measured by measuring contact angle for different applied voltages. A novel technique for direct measurement of Electrowetting Force (EWF) using nano indenter is proposed in this work. The EWF measurements show that, for aqueous solution the EWF is more as compared to DI water. Additionally, the electrowetting system is found to be more susceptible for degradation when aqueous solution is used. The performance degradation due to defective dielectric layer is also investigated by measuring the electrowetting force. Degradation of EWOD systems with environmental exposure over time is further studied experimentally by contact angle and electrochemical impedance spectroscopy (EIS) measurements. The time constant of 'contact angle decay' with environmental exposure is found to be similar to the time constant of electrolyte diffusion in dielectric layer.

CHAPTER 1 INTRODUCTION

1.1 Thesis Statement

The thesis will address the characterization methods of electrowetting systems response. A novel technique of measuring capillary forces in electrowetting system and investigate the reliability of electrowetting systems. The electrowetting system response for different parameters such as liquid type, voltage type and voltage polarity is characterized by contact angle and electrowetting force (EWF). The liquid exposure effects on electrowetting system response are examined by measuring the contact angle. The electrochemical impedance spectroscopy is used to investigate the electrochemical corrosion in electrowetting systems.

This chapter will review the motivation and scope of this research work.

1.2 Motivation

In last two decades microfluidic devices have been investigated and numbers of products are already available on the market. The manipulation of small liquid droplets has been used in most of the Microfluidic devices. The application of microfluidics includes continuous flow of liquid, individual droplet movement, DNA chips, molecular biology, tunable micro lenses, acoustic droplet ejection, fuel cells and more.

Electrowetting is a powerful actuation mechanism in which the surface energy of a fluid is being changed by applying electrical energy. Electrowetting has been

used in a number of applications from digital microfluidics to displays. The transport of liquid droplets on an array of electrodes has been demonstrated by Sung et al [1, 2]. The mixing of droplets and inducing a chemical reaction based on electrowetting has been demonstrated by Pail et al. and Fowler et al. [3, 4]. Electrowetting based optical switches have been demonstrated by Yang et al [5] .Thermal management of electronic devices by liquid cooling have been investigated in recent years [6-10]. Mugele et al. [11] reported transport and mixing of droplets for printing. Chen et al. [12] used electrowetting for suction of liquids in microtubes.

Electrowetting based optical devices are commercially available. The difference in the refractive index of various liquids has been used as the basic aspect for electrowetting based tunable micro lenses. In 2000, Berge et al. [13] reported the tunable micro lenses based on electrowetting principle. The authors used non-polar oil droplet and salt solution in a closed cell and used the difference in refractive index along with contact angle difference for controlling the focal length of lenses. Later Krupenkin et al. [14] reported similar tunable micro lenses with a lateral positioning option of lenses. In 2004, Kuiper et al. [15] reported the tunable lenses with integrated CCD cameras for a cell phone display. Hayes et al. [16] reported the use of electrowetting in display technology by using oil droplet having colored die and slat solution on predefined and patterned electrodes. Later, Heikenfeld et al [17, 18] and Roques et al. [19] also reported electrowetting based display. Liquavista Inc. commercially launched the electrowetting based display in 2006.

1.3 Scope of Work

The electrowetting based systems have been proven to have a great importance in commercially available products. The design and characterization of such electrowetting actuated devices will need to focus on exploiting device scaling while optimizing for reliability and lifetime. However, many microfluidics researchers have acknowledged unexplained behavior and performance degradation. These include spurious droplet motion, oscillations, voltage polarity dependence, and sensitivity to the ambient medium [20-29].

The characterization of electrowetting system is often carried out by contact angle measurements due to simple equipment configurations, direct wetting angle measurements and large body of comparative measurements. However, the accuracy and response time of system of contact angle measurement is limited. Verheijen et al [30] experimentally measured the capacitance of electrowetting systems. The measurements were repeatable but the response time of the measurements was similar to contact angle measurements.

In this work a novel technique for direct measurement of capillary forces in electrowetting has been investigated. The electrowetting force (EWF) has been measured by a modified Hysitron Triboindenter. The effects of different parameters of interest such as voltage type, voltage polarity and liquid type in electrowetting system have been investigated.

Additionally, due to the functional nature of electrowetting in liquid environment with different ions, dielectric materials and strong electric field make the system prone for electrochemical corrosion and could further degrade the performance of

the system. However, due to compact nature of electrowetting system the electrochemical corrosion has been never investigated before. In this work, the Electrochemical Impedance Spectroscopy technique has been used to study corrosion in the electrowetting system.

1.4 Thesis Outline

This thesis proceeds as follows: Chapter 2 reviews the previous work done on electrowetting processes and summarizes their outcomes. Chapter 3 details the experimental technique used in this work for characterization of electrowetting. Chapter 4 discusses the experimental results of contact angle measurement and electrowetting force measurement and compares the variations due liquid type and voltage polarity. In chapter 5, the affects of environmental exposure on electrowetting system is reported. Chapter 6 concludes the work done and recommends future aspects for improvement and optimization of the electrowetting processes.

CHAPTER 2 LITERATURE REVIEW

2.1 Wettability

The behavior of any liquid droplet over a surface is known as the 'Wettability' of the liquid and surface. When a liquid droplet is kept over a surface, how well it sticks or spreads depends on the wetting characteristics of the droplet and the surface. The interaction between a liquid droplet and surface droplets is often characterized by a contact angle. Consider the case of a liquid droplet on a surface, the possible shape of the droplet on a surface is shown in Figure 1.

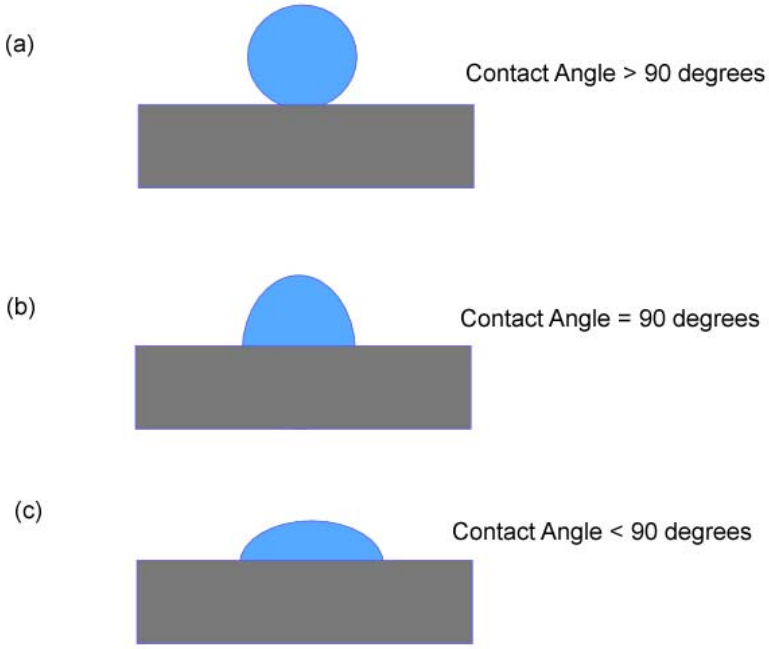

Figure 1 Possible Shapes of a Droplet on a Surface

The fundamental phenomena of contact angle and wettability can be described by the Young equation. Figure 2 shows the three phase contact line and the Young equation can be expressed by following equation,

$$\gamma_{SV} - \gamma_{SL} = \gamma_{LV} \cos\theta$$

Equation 1. Young's equation for interfacial tensions

where γ stands for interfacial energy and S,L and V stands for solid, liquid and vapor respectively and θ for contact angle.

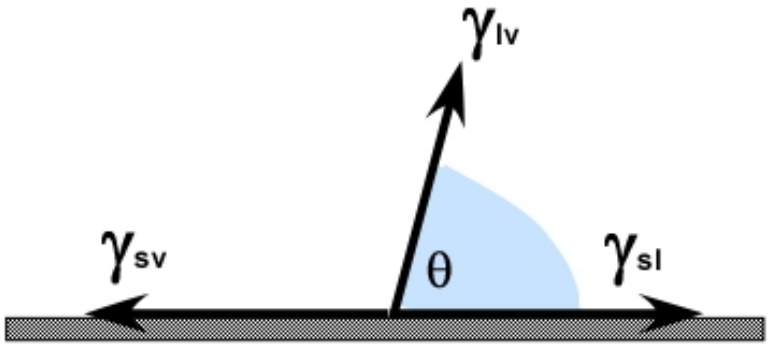

Figure 2 Young Equation for Three Phase Interfacial Tension.

2.2 Electrowetting

Miniaturization increases surface to volume ratios bringing more challenges in control of surface and surface energies [23]. In 1875, Gabriel Lippmann demonstrated a relationship between electrical and surface tension phenomena. This relationship allows efficient control of the shape and motion of a liquid meniscus by applying a voltage. The liquid changes shape when a voltage is applied in order to minimize the total energy of the system (sum of surface tension energy and electrical energy). Today, this effect, known as electrowetting, has shown potential importance in many applications.

The idea behind electrowetting is to make the surface highly wettable by an applied electric field. In electrowetting on a dielectric, the change of contact angle as a function of the applied voltage can be related to the dielectric thickness (δ) and dielectric strength (ε_R) as proposed by the Young- Lippmann equation [23].

$$\cos\theta_1 = \cos\theta_o + \frac{\varepsilon_o \varepsilon_r V^2}{2\gamma_{lv}\delta}$$

Equation 2 Young-Lipmann equation

It employs control of voltage that changes the interfacial energy of the liquid-solid interface [23]. By alternatively applying voltage across an electrode, the fluid can be efficiently moved as desired, by changing contact angle of the liquid on the surface. This is proved by many works done so far by applying large voltage on dielectric called Electrowetting on Dielectric (EWOD) that provided large changes in the contact angle.

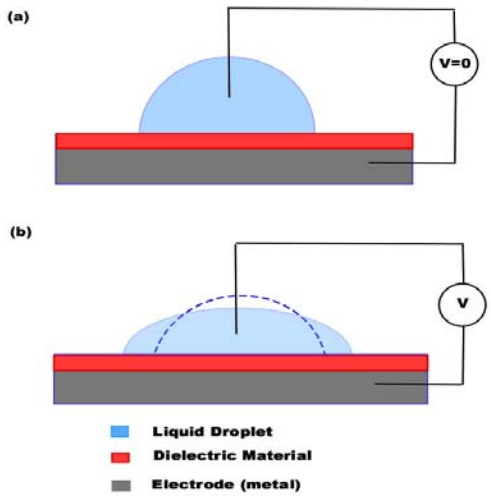

Figure 3 Electrowetting of a Droplet. Basic Principle Demonstration

Figure 4 shows most common configurations employed in the electrowetting phenomenon. In the grounded droplet method, the liquid is grounded while in the floating droplet, the droplet floats across two electrodes with applied voltage across them.

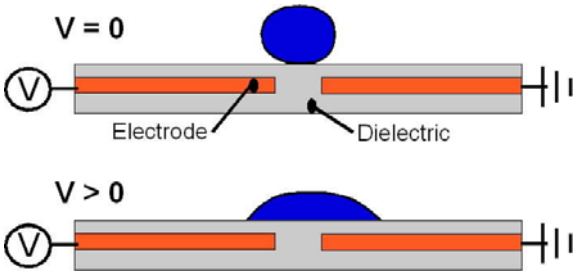

Figure 4 Electrowetting of a Droplet. A Coplanar Electrodes Configuration.

2.3 Contact Angle Variation

There is a considerable amount of literature on contact angles and wetting phenomena [21, 23, 24, 26, 31-33]. The voltage applied between the droplet and the counter-electrode generates electric charges on both conducting surfaces. The mechanism of charge generation, and its distribution, can be rather complicated for real electrolytes, but the assumption of an ideally conducting fluid with a surface charge density is usually sufficiently accurate. The Young-Lippmann equation predicts a near parabolic curve for a sessile drop on a single dielectric plate, relating contact angle to the capacitive voltage across the plate. One of the Electrowetting objectives is to maximize the accessible contact angle range. Contact angle decreases to a minimum value upon applying the voltage. Minimum contact angle is known as '*Saturated Contact Angle*' and corresponding voltage is known as '*Saturation Voltage'*. A reasonable amount of research was done to find out the contact angle saturation phenomena [24, 31]. Verheijen and Prins [26] found indications that the insulator surfaces were charged after driving a droplet to contact angle saturation. They suggested that charge carriers are injected into the insulators. These immobilized charge carriers then partially screen the applied electric field. It seems clear that diverging electric fields at the contact line can induce several distinct non-linear effects and each of them may independently cause saturation. Which

effect dominates depends on the specific conditions of each experiment and identifying these conditions requires more work in the future.

Quinn et al. [24] studied contact angle saturation in electrowetting. The saturation of contact angle was related to the magnitude of the capillary force variation. Also contact angle saturation phenomena are related to the materials properties. Above the contact angle threshold the electrowetting phenomena is considered to be the non equilibrium process.

2.4 Contact Angle Hysteresis

Contact angle hysteresis is another piece of the boundary physics needed to complete the model of droplet motion using EWOD forces. Hysteresis refers to the difference in contact angles between the advancing and receding ends of sessile drops [34]. It is a direct consequence of contact line pinning, which acts as a force that resists any sliding motion, and it can be seen when water droplets stick to the side of a solid surface. For a sessile drop on a single plate, it can be seen that the advancing and receding contact angles are greater and smaller, respectively, than the nominal contact angle. The contact angle of the droplet and contact angle hysteresis is strongly influenced by the surface morphology. Bhadur et al. [35] studied the electrowetting on the rough surface. Analysis was done based on the minimization of energy. Dynamic electrowetting based on the surface design was proposed.

2.5 Material Properties

In basic Electrowetting theory the liquid droplet is considered as perfect conductor. The requirements regarding the concentration and nature of charge carries are

not strict. Most authors report no affect of concentration of salts in the liquid on the electrowetting. On the other hand the properties of insulating layer are much more critical. Substantial work has been done to optimize the insulating layer thickness and properties of the insulating layer for low voltage electrowetting. The two criteria for insulating material optimization can be obtained from the Young-Lipmann equation. First one can obtain maximum contact angle at zero voltage and second criteria should be the possible minimum insulating layer thickness. The minimum thickness of dielectric layer will lead to a high capacitance value and accordingly the contact angle modulation will be high. The first choice can be met by hydrophobic insulating polymer.

Thin layers of amorphous fluoropolymer (Teflon or CYTOP™ or Paralyne) are often used. These organic compounds can be easily deposited with thickness ranging from few nanometers to micrometers range by spin coating or dip coating methods. The commonly used inorganic compounds for dielectric layers are silicon dioxide and silicon nitride. In general, thin film deposition technique is being used for inorganic dielectric layer. To make surface hydrophobic, a thin layer of hydrophobic compound is coated over the inorganic substrate.

Seyrat et al. [34] in 2001 reported on the different thickness of amorphous fluoropolymer used and their critical effect on the reversible electrowetting. Coatings dried at room temperature are typically observed to have reduced electrowetting modulation (i.e. difference between the contact angle at zero volts and saturated contact angle) and fewer adherences to the electrowetting theory.

Peykov et al. [32] studied the electrowetting with parylene and Teflon dielectric layers with thin gold film as electrode. A double layer effect was studied in depth and

theoretical model was developed for the contact angle saturation. The model proposed in this work predicts that for an electrowetting device in which an aqueous droplet can be forced to completely wet a hydrophobic surface, a surface with the same surface energy as the liquid is required. Indeed the work presented a more detailed consideration of electrowetting taking into account the structure of the double layer.

Moon et al. [36] in 2002 reported low voltage electrowetting. Three different types of dielectric layers namely, Teflon, silicon dioxide and Parylene with varying thickness was studied. A contact angle modulation of 40° was reported for the actuation voltage of 15V.

Cahill et al. [37] studied the platinum and copper electrodes for EWOD experiment. The leakage current and resistance were measured experimentally to characterize the dielectric materials. Breakdown voltage tests were performed for Parylene C and SiN.

Raj et al. [38] studied the composite dielectric materials for low voltage electrowetting. The composite dielectric was made of aluminum oxide and silicon nitride. CYTOP™ was spin coated over the composite dielectric to make surface hydrophobic. The aluminum oxide, thickness of 100 nm, was deposited by atomic layer deposition. Later, silicon nitride (thickness of 150 nm) was deposited over the aluminum oxide using plasma enhanced chemical vapor technique. To reduce the contact angle hysteresis, the electrowetting experiment was carried in dodecane oil environment. The authors reported the optimal thickness of the CYTOP™ to be 50 nm for nominal electrowetting actuated devices. The CYTOP™ thickness greater or lower than 50 nm may cause charging in dielectric layer.

Banpurkar et al. [39] reported the electrowetting of aqueous gelatin material in the form of a small droplet over Teflon coated substrate. The authors explored the possibility of the electrowetting of soft matter materials for inner sight of the rheological properties of such materials in liquid phase.

2.6 Effects of Gravity and Evaporation

Another consideration when using a single-plate design is the effect of gravity on the motion of large drops. The ratio of gravitational to surface tension forces is characterized by the Bond number. Although it is not clear at what Bond number gravity affects electrowetting translation, a Bond number of unity corresponds to a droplet volume of 82 µl for water [21]. Thus, for maximum EWOD applications droplet volumes correspond to Bond numbers much less than unity and are therefore typically small enough that surface tension dominates gravitational forces.

With the droplet exposed to the ambient air, one must consider evaporative losses of the droplet. Chen et.al. [21] reported that a 5 µl droplet requires 33 min. to evaporate from a Teflon surface under a laminar flow hood. It is observed that droplets on hydrophobic surfaces such as Teflon have a longer evaporation time than droplets on hydrophilic surfaces. When the droplet is protected from air flow, the evaporation time can be substantially increased. In the same article, they claimed that in a zero humidity environment, a 250 µl droplet takes 7 minutes for evaporation. For many microfluidic applications and testing done in this work, this time span is sufficient.

2.7 Electrowetting Characterization

Baviere et al. [40] reported dynamics of droplet actuated by electrowetting in air. The transportation of small volume droplets were investigated by stroboscopic observations. The effect of viscosity on the droplet velocity with the varying voltage was studied. The electrowetting actuated droplet velocities were found highly sensitive with the viscosity of fluid. A high velocity of 114 mm/sec with the actuation voltage of 100V was reported.

Baird et al. [33] proposed a method to examine electrostatic force on microdroplets transported via Electrowetting on Dielectric (EWOD). The force distributions on advancing and receding fluid faces are detailed in each case. Dependence of the force distribution and its integral on system geometry, droplet location and material properties are described. A comparison of scaling properties and force distribution for both cases are given. The effect of the divergent charge density on possible explanations for contact angle saturation such as charge trapping, local dielectric breakdown, and corona discharge were studied. Both analytical results for integrated total forces and numerical results for the force distribution were compared and proven to be in agreement.

Walker et al. [41] discussed the modeling and simulation of a parallel electrowetting on dielectric device that studied droplet movements through surface defects. The simulations were compared to that of the experiments for a splitting droplet various factors affecting electrowetting effects were. The governing fluid equations and boundary conditions along with contact hysteresis were developed. A numerical simulation was described which uses a level set method for tracking the droplet boundary.

Berthier et al. [42] proposed a technique to find to investigate minimum and maximum actuation voltages in electrowetting. He formulated maximum voltage as a threshold beyond which there is no more gain in the capillary effect due to the saturation. Calculation was done to determine the electrowetting force on a EWOD system considering the contact angle hysteresis and an analytical relation was obtained to derive the minimum actuation potential.

Verhejen et al. in 1999 [26] reported the effect of trapped charges on the EWOD. The experiments were conducted on silicon substrate with aluminum (100 nm thickness) as electrode, an insulating layer of Parylene C (10μm thickness) and a thin hydrophobic layer AF 1600. The EWOD experiments were conducted inside the silicone oil to reduce the contact angle hysteresis. The 10 μl sized aqueous solution potassium chloride and potassium sulphate was used for EOWD testing. Verhejen et al. [26] reported that up to a threshold voltage, the charge remains in liquid and is not trapped. However, once the threshold voltage is reached, then interaction of ions inside the liquid has more attraction towards the solid as compared to liquid. A modified Young Lipmann's equation accounting for the trapped charges was proposed. Later, contact angle was estimated from the capacitance values of EWOD system using the modified Young - Lipmann equation.

CHAPTER 3 EXPERIMENTAL PROCEDURES

3.1 Introduction

The characterization of the electrowetting on dielectric (EWOD) in this work has been done by multiple experimental techniques. In this chapter, the basic principle, experimental set up and procedures are discussed in detail.

3.2 Sample Preparation

All experiments in this work are carried out on silicon wafers. All fabrication steps were done at Nanomaterials and Nanomanufacturing Research Center (NNRC) facility at USF.

First of all, a silicon dioxide layer of ~500nm is thermally grown over Si wafer. Thereafter a ~ 300nm thick Al metal thin film is deposited by sputtering process. Further fabrication process depends on the experiment of interest. For the contact angle measurement and EIS experiment, a thin amorphous fluorocarbon polymer (CYTOP™, Asahi Glass Co., Ltd) is spin coated which works as a dielectric and hydrophobic layer. In this work, all the samples are coated with two layers of CYTOP™. Two layers of CYTOP™ have fewer defects as compared to a single layer. Two layers of CYTOP™ is spin coated on almost $3/4^{th}$ of the Si wafer surface except for ~1.5 cm near the flat edge of the wafer to make electrical connection with the aluminum electrode as shown in Figure 5. After the first coating of CYTOP™ wafers were baked at 90°C for 30 minutes

in a conventional oven. Then a second layer of CYTOP™ is spin coated and final baking is done at 150°C for 1 hour.

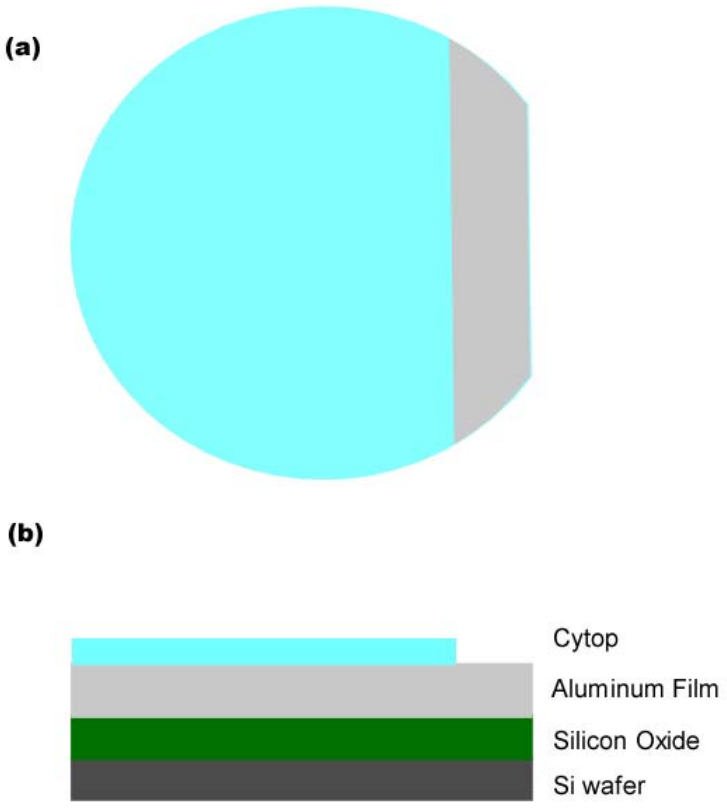

Figure 5 Top View of the Sample and Stacked View of the Sample Used for Contact Angle Measurement and Electrochemical Impedance Spectroscopy

For electrowetting force measurement, coplanar electrodes were patterned. After the aluminum film deposition, Shipley 1813 photoresist was spin coated and baked on a hot plate at 90°C for 90 seconds. Thereafter, using the mask aligner, photoresist coated wafers were exposed to UV light for desired pattern. Then the sample was developed using MF319 developer to develop the pattern exposed by UV light. Wet etching technique was used to etch the aluminum and make coplanar electrodes. The aluminum etchant was heated to 60°C in a beaker and developed samples were immersed in etchant

for 30 seconds. Then wafers were rinsed in DI water and dried. Later, solvent (ethanol and methanol) were used to strip off the photoresist with a result shown in Figure 6. Then two layers of CYTOP™ were spin coated and baked.

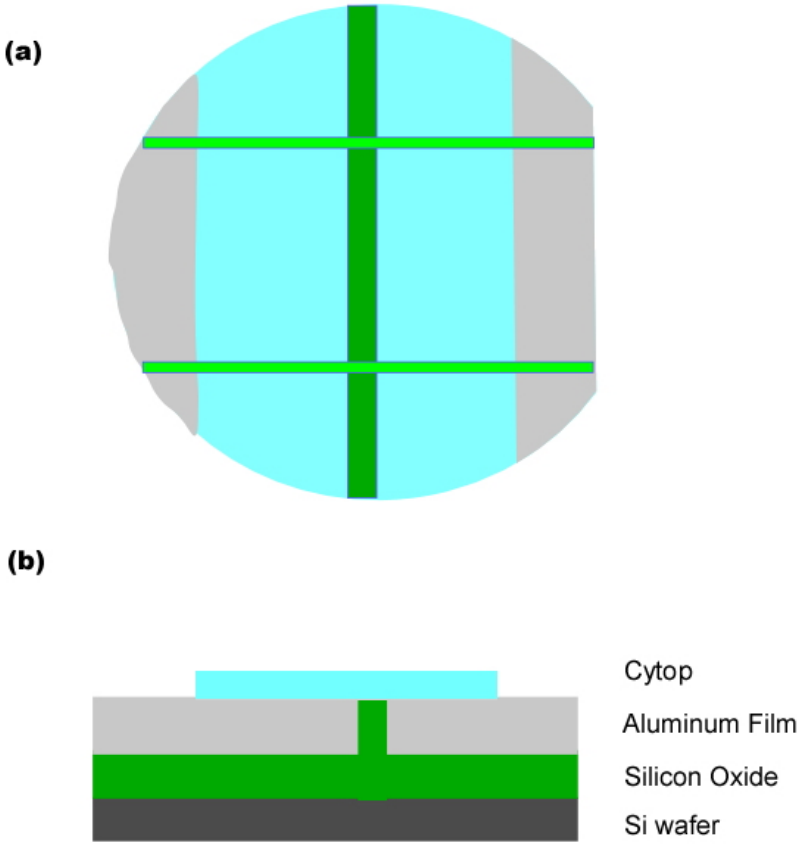

Figure 6 Top view of the Sample and Stacked View of the Sample for Electrowetting Force Measurement.

The thickness and roughness of CYTOP™ film were measured by the step profilometer and used in all analysis. The electrical connections across the electrode

during the experiment are made by putting conductive copper tape on the aluminum film near the edge.

3.3 Contact Angle Measurement

Contact angle measurement (CA) is a simple technique for measuring the wettability of liquid and surface. In general surface energy is measured by two different methods, namely, goniometry and tensiometry. In goniometry, a goniometer is used for the direct measurement of contact angle. The analysis of contact angle is based on the shape of the droplet in goniometry. The contact angle is measured by drawing a tangent at the edge of droplet and surface interface. In tensiometry the interfacial energy is found by measuring the attraction force between solid and liquid droplet provided geometry of solid and surface tension of liquid are known. The contact angle analysis of fibers is often done by tensiometry.

The change in contact angle with voltage in electrowetting can be captured using goniometer due to small-sized droplets. In this work, a Ramehart Inc. (model number: 100-00-115) goniometer is used for the contact angle measurements.

3.3.1 Method

The contact angle is measured by sessile droplet method. In the measurement the following assumptions are made: first the drop is symmetric about vertical axis and secondly, droplet is in not moving. The droplet size is kept in the range of 5-10 micro liters, to reduce the effect of gravity. In this way, the measurement of contact angle leads the measurement of interfacial energy between droplet and surface.

The goniometer available in the lab has movement in all three axes. Before any experiment, the panel is aligned to be flat and calibrated accordingly. The dispensing of a

droplet on substrate is done precisely by a micrometer syringe having micro liter resolution. The syringe is attached to the clamp, and the droplet is released along with the upwards movement of panel (attached to goniometer) containing substrate, until the droplet touches the substrate. The manual dispensing of droplet on substrate needs to be done carefully to avoid the scratch in the substrate. Then by moving the panel along X and Y axis, droplet is focused for accurate measurement. Thereafter, by moving the panel in X direction, the edge of droplet is located and contact angle is measured directly along the tangent at the edge of droplet and surface shown in Figure 7.

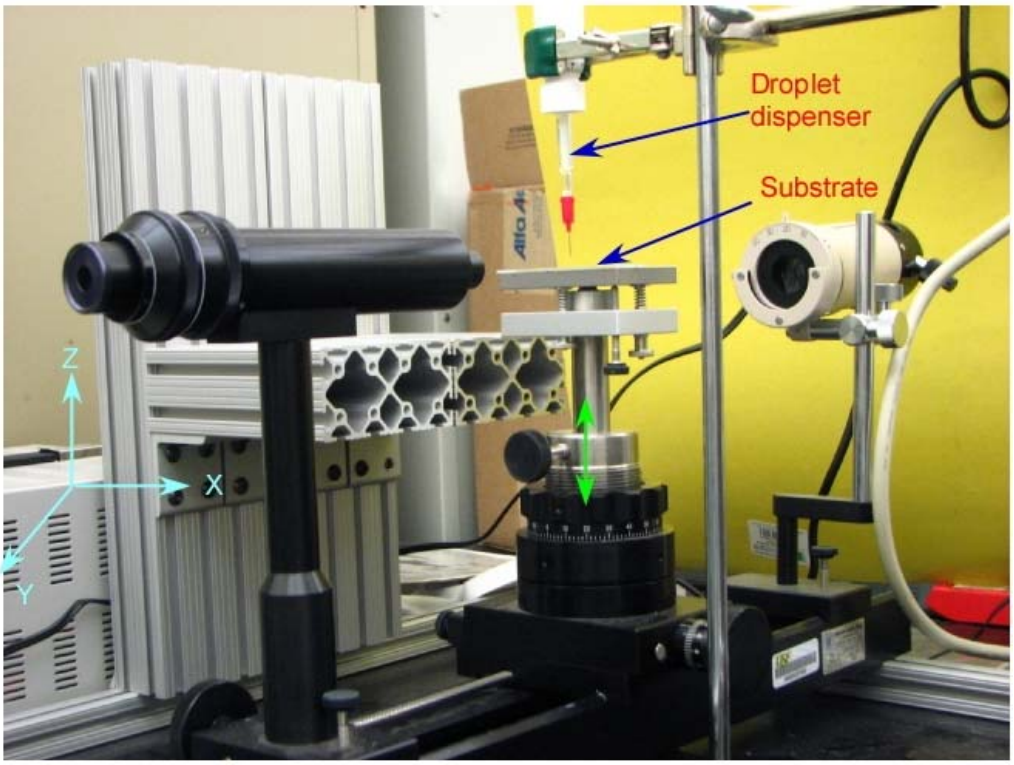

Figure 7 Contact Angle Measurement Set-up. A Goniometer is Used for Measuring the Contact Angle Using Sessile Drop Method.

For electrowetting experiments, a wire electrode is dipped half way inside the liquid. The copper tape is attached to the aluminum film. Then alligator clips were attached to wire electrode and copper tape connected to the power source. The polarity of electrodes can be changed simply by changing the position of alligator clips attached to the power source. The

voltage output of the power source can be changed by a knob attached to the machine. During the electrowetting experiment, first the contact angle is measured without any voltage applied. Then, voltage was applied small steps (5-10V) and contact angle were measured. After measurement, the voltage output was kept off and contact angle was measured again to investigate the hysteresis of electrowetting.

The contact angles measured in lab have tolerance of +/-2° as the measurements can be performed only manually.

3.4 Electrowetting Force

3.4.1 Introduction

Electrowetting is an effective method to manipulate droplets in Digital Microfluidics. The forces induced due to the principle of electrowetting is the main source of control of these droplets by causing an apparent change in the surface energy due to the voltage applied across the substrate on which the droplet is located. These forces can greatly affect the performance of electrowetting devices. Therefore, force measurement and optimization are critical to process improvements. A novel method has been developed to measure these forces in two-dimensions.

3.4.2 Principle of Electrowetting Force Measurement

In the case of interest, the drop is positioned over two electrodes with a voltage difference across the electrodes. The electrodes are covered with a dielectric material. The droplet can be considered conductive so that the system is modeled as two capacitors in series. The electrowetting configurations are shown in Figure 8.

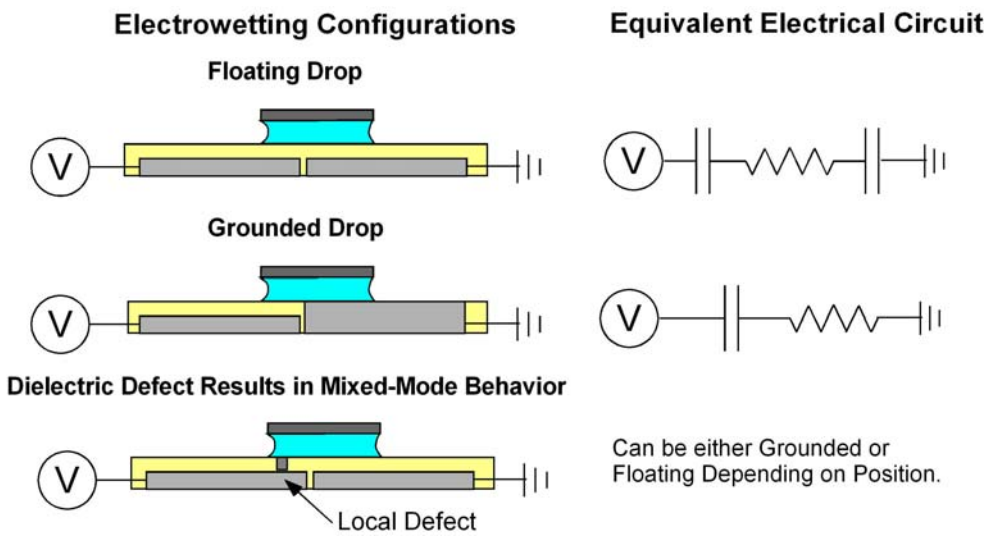

Figure 8 Electrowetting Configurations and Equivalent Electrical Circuit

The voltage between each pad and the drop will vary as the position of the droplet changes due to changes in the capacitor area and thus their capacitance. Neglecting the droplet resistance, the arrangement can be modeled as simple series capacitor circuit composed of two parallel plate capacitors. The voltages across the left and right capacitors (V_L, V_R) are given as:

$$V_L = \frac{A_R}{A_L + A_R} V_{tot}$$

Equation 3. Voltage across left capacitor

,

$$V_R = \frac{A_L}{A_L + A_R} V_{tot}$$

Equation 4 Voltage across right capacitor

The change in contact angle is driven by the reduction in effective surface surface energy by the energy stored in the capacitors. Using these relationships, the total capacitive energy is given by

$$E = \frac{1}{2}\left(C_l V_L^2 + C_R V_R^2\right)$$

Equation 5. The total energy stored in capacitor

The area of the droplet over each electrode (A_L, A_R) is a function of the droplet position and the form of this function depends on droplet shape. In general, this shape will vary with the offset from the equilibrium position. If the droplet is kept middle between the coplanar electrodes, then the system remains in equilibrium. However, if the droplet is offset from the equilibrium position, the droplet tend to move other side (not towards the offset side Figure 9).

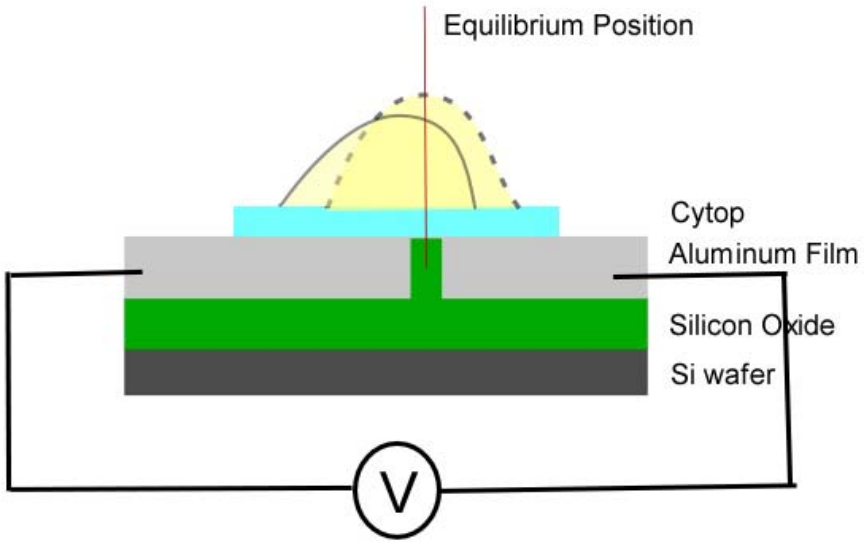

Figure 9 The Equilibrium Position and Offset Position of Drop on Coplanar Electrodes During Electrowetting Experiemnt

In the EWF experiment, the droplet is sandwiched between the substrate and an electrically insulating coverplate that is wet by the fluid, the droplet contact area and shape on the substrate will approach the area of the coverplate as the droplet thickness decreases relative to the coverplate dimensions. With this simplification, the area values of the droplet beneath a square coverplate with edge length s can be related to the displacement (x) of the coverplate from the equilibrium position.

$$A_L = s\left(\frac{s}{2} + x\right),\ A_L = s\left(\frac{s}{2} + x\right),\ -\frac{s}{2} < x < \frac{s}{2}$$

The energy and force as a function of position is then

$$E = \frac{V_{tot}^2 \varepsilon_0 \varepsilon_R}{8\delta}\left(s^2 - 4x^2\right)$$
$$F_x = \frac{dE}{dx} = -\frac{\varepsilon_0 \varepsilon_R}{\delta} V_{tot}^2 x$$

Equation 6. The energy of the system and predicted model of electrowetting force

where the force as a function of cover plate position is found by differentiating the energy E with respect to the displacement x. The static equilibrium position is at the center of the two drops with equal area on each electrode. In cases of limited viscous and electrical energy loss, the drop could oscillate around the equilibrium when disturbed.

Another behavior that can be observed during electrowetting is induced by the presence of a hole in the dielectric layer. A hole would short the capacitor on one side so that no voltage will be applied across the region of the drop over the shorted electrode. The full voltage drop will occur across the other side. In this case, the electrowetting force will be constant with displacement. It is given by:

$$F_x = -\frac{\varepsilon_0 \varepsilon_R}{2\delta} s V_{tot}^2$$

Equation 7. The electrowetting force for a sorted capacitor

3.4.3 Experimental Setup for Electrowetting Force Measurement

This was implemented by attaching a 9mm x 9mm glass plate to a modified tip of a Hysitron Triboindenter in Figure 10. The assumptions made in this technique are:

- Wetted indenter plate.
- Very thin fluid so that substrate contact area closely approximates the indenter plate area.
- Fluid fully wets the entire substrate area.
- The indenter plate and substrate are parallel.

The Triboindenter measures the forces on the plate normal to the substrate and in one in-plane direction.

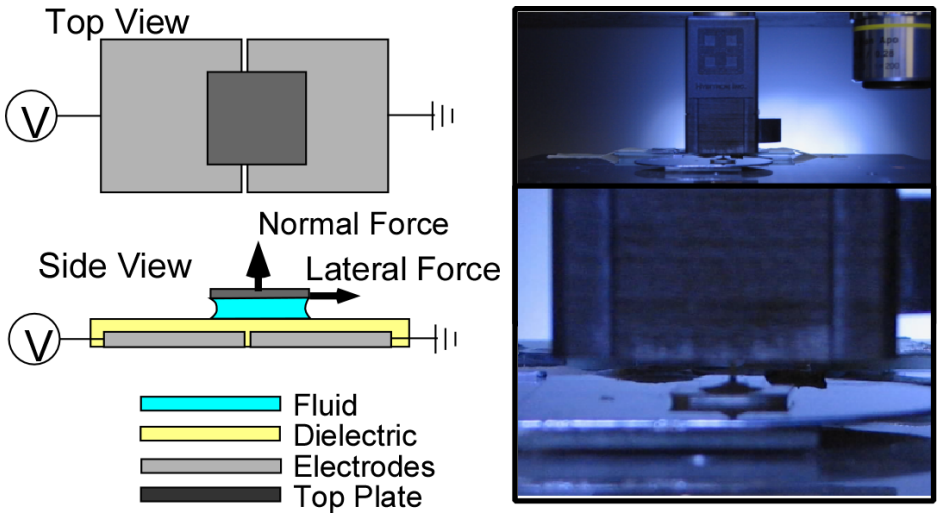

Figure 10 Schematic of Electrowetting Force Measurement and Picture of Experimental Set-up

Since water wets the glass plate, drops are trapped between the plate and the substrate. As the gap between the plate and substrate decreases, the drop/substrate

contact area closely approximates the area of the top plate and is does not change significantly under an applied voltage.

3.4.4 Experimental Procedure

For EWF measurements, the substrate with conducting tape attached for electrical connection is placed on the panel. The coordinates of the position near the edge along gap is measured and alignment of gap is checked. If the sample is misaligned in any of direction then sample is tilted such that gap looks perfect horizontal. Then coordinates of the gap is found. The coordinates of gap center is needed for positioning the droplet The droplet position located at the 3mm offset from the gap center in all experiments until stated otherwise. Then droplet size of 50-55µL is placed on the defined position. The alligator clips were connected to conducting tape attached with metal electrode on the substrate. Then the coverplate attached tip is lowered down and droplet is squeezed. The droplet is squeezed until the coverplate is wetted completely. Before every test the air scratch is done to obtain the lateral and normal force. For WEF measurements it is necessary to minimize the drift before applying the voltage across the electrodes. The normal drift data less than 300µN for a 15 seconds air scratch test is considered good for testing. Additionally, the minimal drift force shows that the coverplate is wetted entirely. Then voltage across electrodes is applied and test is performed.

3.5 Electrochemical Impedance Spectroscopy

3.5.1 Introduction

The use of aqueous droplet in electrowetting actuated applications was reported earlier**.** For any electrochemical reaction, such as corrosion, to takes place water, oxygen

and ionic flow are required. The use of the organic coating in electrowetting applications acts as a dielectric layer also. The organic coating in general shows very poor ionic conductivity. However, in two conditions the organic coating, CYTOP™ which is in interest of this work, could possibly provide an ionic path. Firstly, pores/defects on the coating can lead to the direct contact of liquid and metal and secondly the diffusion of water into the polymer in contact. The possibility of discussed two mechanisms is very likely in electrowetting phenomena.

The investigation of coating performance *in situ* environment requires a non-destructive technique. Electrochemical impedance spectroscopy (EIS) has been proven to be a powerful technique in corrosion characterization.

3.5.2 Principle of Electrochemical Impedance Spectroscopy

A metal with a flawless organic coating on its surface tends to behave similarly as an ideal capacitor with capacitance C,

$$C = \frac{\varepsilon \varepsilon_0 d}{A}$$

Equation 8. Capacitance of a metal with organic coating

where C is the capacitance, ε is the dielectric constant of organic layer, A is the area and d is the thickness of the organic layer. The dielectric constant of a polymer coating is a value typical of polymers (ε ~2 to 5). In this work, the dielectric constant of organic polymer is 2.1. However, as electrolyte molecules are absorbed by the coating during service, the dielectric constant increases because of the much higher dielectric constant of water.

The dielectric constant of the polymer with an absorbed water volume fraction, *f,* as,

$$\varepsilon = f \times \varepsilon_{CYT} + f \times \varepsilon_{W}$$

Equation 9. Change in dielectric constant with water absorption.

where ε_{CYT} is the dielectric constant of the polymer (CYTOP™ in this work), ε_w is the dielectric constant of water. Because of the high value of ε for electrolyte, ε increases with the immersion time [43]. For water, the percentage of water volume fraction, *f,* diffused in the polymer can be found as,

$$\varepsilon = \varepsilon_{t=0} \times 80^{f}$$

Equation 10. Change in dielectric constant of cytop with water absorption.

The "diffusion" of water molecule in the polymer coating can be expressed by Fick's first law of diffusion as [44],

$$x = \sqrt{D \times \tau}$$

Equation 11. The relation between diffusivity constant and time constant

where x is the thickness of the coating, D is the diffusivity coefficient of sodium chloride solution in polymer and τ is the characteristic time .

In electrowetting, the dielectric layer is exposed to the liquid droplet over long periods of time. If the dielectric and droplet interacts, this creates a situation where the capacitance of the dielectric layer changes with time. This could have the adverse affects on the performance of the electrowetting. The reliability of electrowetting system due to electrochemical corrosion has been discussed previously, but the proper investigation has

not been carried out so far. In this thesis, the EIS for investigation of electrowetting system reliability has been explored.

3.5.3 Experimental Procedures

The EIS requires there electrodes namely, working electrode, counter electrode and reference electrode. The working electrode is submerged in the electrolyte during test where as the counter electrode provides the connection to metal beneath the coating for impedance measurement.

In this work, the design of the electrochemical cell has been adopted from Sagues et al. [45]. The schematic of electrochemical cell is shown in Figure 11. The experimental set up is shown in Figure 12. A plexi glass tube of 1.5 inches in length (outer diameter d= 3.2 cm, inner diameter = 2.5cm) is glued with epoxy (Loctite made, 3 minute adhesive) on the CYTOP™ spin coated Si wafer. The tube is glued over the CYTOP™ part of the Si such that counter electrode connection can be easily made near the flat edge of the wafer which is only coated with aluminum thin film. Activated Titanium (coated with metal oxide such as Tantalum, Niobium and Zirconium oxides) wire is used for the counter and reference electrodes. The cell attached with the wafer is then placed over the plexi glass sheet. All three electrodes are then connected with the SS screws as shown in Figure 11. During the experiment, alligator clips of the EIS testing machine is connected with the screws to make connections. Data of the experiment are collected over different time period to observe the effect of diffusion of water and hence the change in capacitance of the coating. Later, using data acquisition system capacitance of the organic coating of the test sample is calculated.

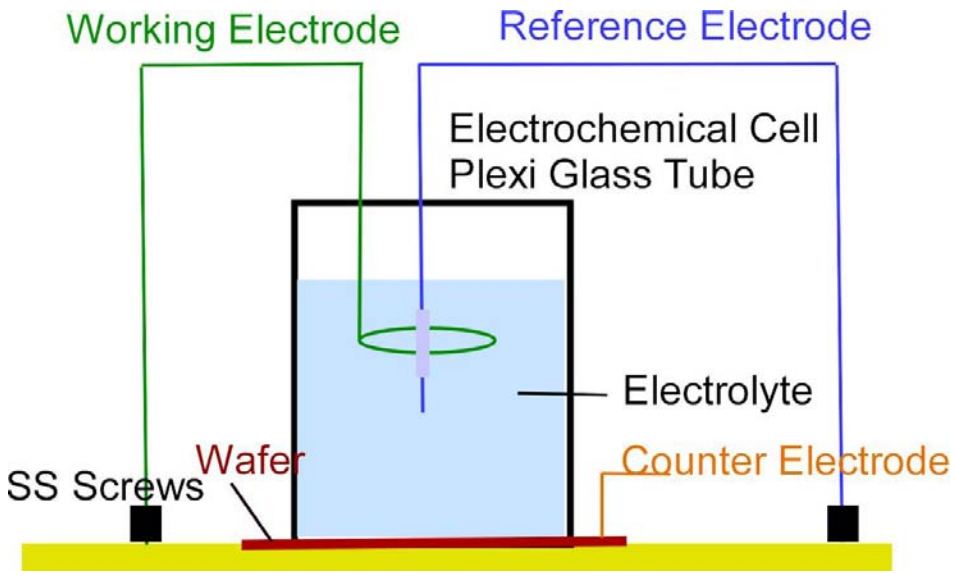

Figure 11 Schematic of Experimental Set-up for EIS Testing

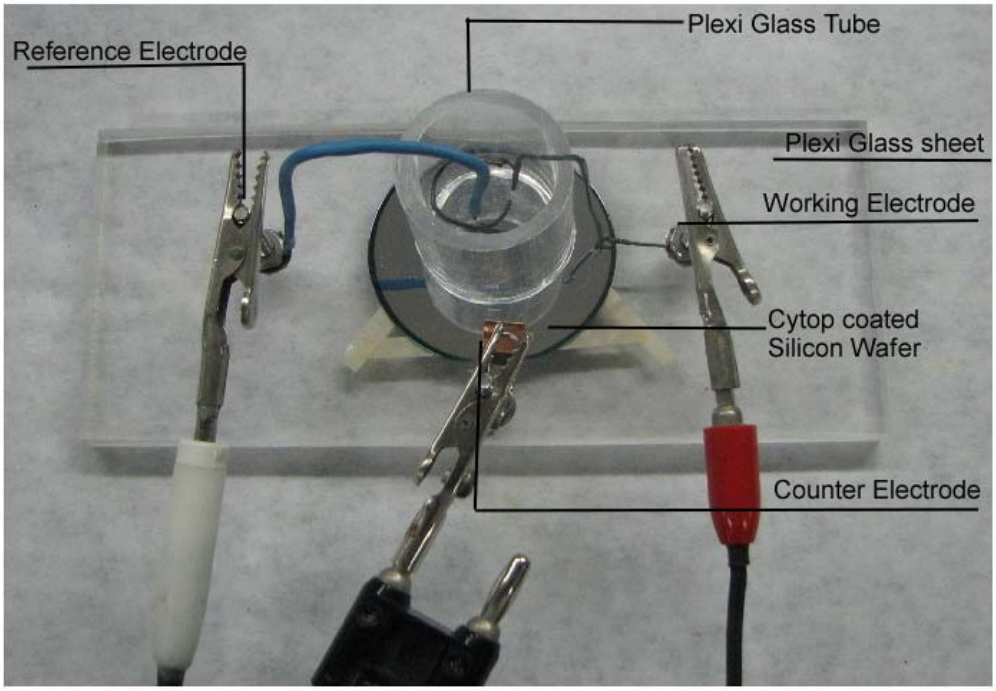

Figure 12 Experimental Set-up for EIS Testing

CHAPTER 4 CONTACT ANGLE AND ELECTROWETTING FORCE MEASUREMENTS

4.1 Introduction

In this chapter, the experimental data are discussed. The first section of this chapter details the contact angle measurement data. Then, electrowetting force (EWF) measurements by modified nano indenter results are discussed. Finally, the electrochemical corrosion observation by EWF measurements are investigated and detailed.

4.2 Contact Angle Measurements

In electrowetting, an electric field is used to tune the interfacial energy and thus droplet shape. The change in shape of droplet upon applying the voltage is measured by change in the contact angle. The electrowetting system is often characterized by the contact angle measurement as a function of varying voltage. In this work, contact angle is measured to investigate the affect of different liquid type and voltage polarity on electrowetting and reversibility of electrowetting process.

4.2.1 Different Liquids

The contact angle is measured for DI water, 1mM NaCl, and 1M NaCl solution. The contact angle is measured using sessile droplet method with droplet size 6-8 μL.

Figure 13 shows the change in contact angle for DI water for sample having 1.78 μm thick dielectric layer. The contact angle changes from 109° to 57°. The contact angle is estimated using the Young- Lipmann equation and plotted with the measured contact angle values. The Young-Lipmann equation observed to be deviating from 30V DC value. The deviation of Young Lipmann equation is not expected at lower voltages. The observed deviation can be due to the error of thickness measurement of the dielectric layer. The adhesive tape was used during spin coating of the CYTOP™ dielectric layer. The tape is used to prevent the coating of dielectric over the aluminum film near the edge where electrical connections are needed for the experiment. The spin coating of CYTOP™ is done at 1600 rpm for 20 second. Due to this, CYTOP™ could accumulate near the edge of the tape. The thickness measurement of the dielectric layer is done by a profilometer. The stylus of the profilometer moves across the edge of CYTOP™ and aluminum to measure the thickness of CYTOP™ film relative to aluminum film. However, the accumulation of CYTOP™ during spin coating and later after annealing treatment can lead to thickness measurement error.

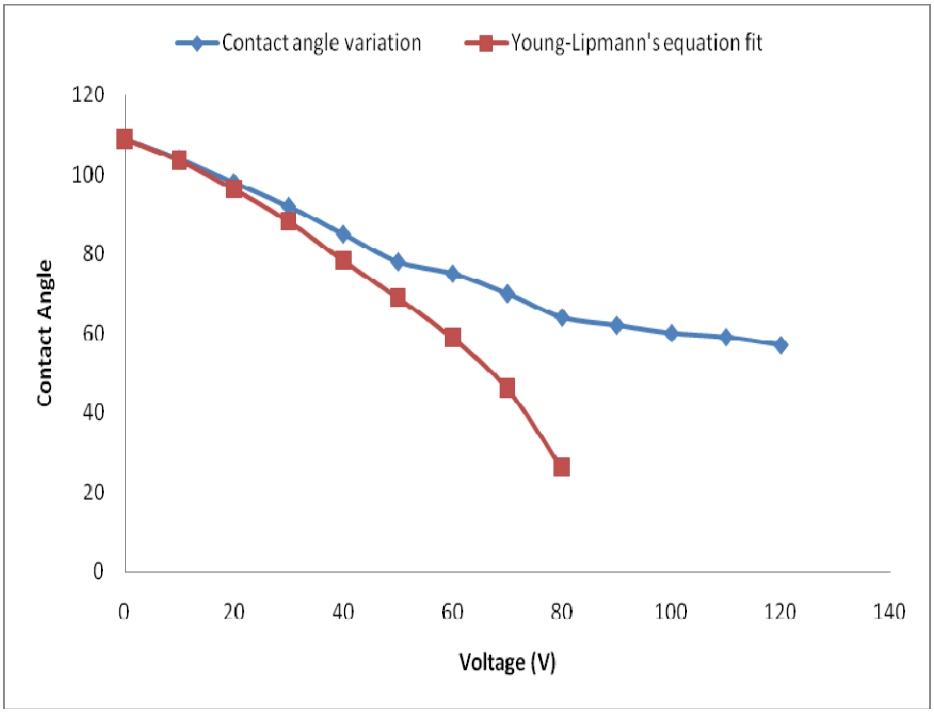

Figure 13 The Variation of Contact Angle for DI Water for DC Voltage. The Thickness of Dielectric Layer is 1.78 µm. The Young- Lipmann Equation is Used to Estimate the Contact Angle at Different Voltages.

Figure 14 shows the contact angle measurement for three different liquids: DI water, 1mM NaCl and 1M NaCl. The contact angle variation is shown in terms of difference in cosine of contact angle at voltage V and voltage zero. The dc voltage was applied up to 120V. The contact angle of the 1M NaCl solution droplet observed to be saturated at 110 V. The 1mM NaCl solution droplet was found to be saturated at 120V. The DI water does not seems to saturated till 120 V. The saturated contact angle for 1mM NaCl and 1M NaCl is found to be 61° and 69° respectively. However, the contact angle measurement at higher voltages needed to justify the saturation of contact angle. The early saturation of 1M NaCl droplet compares to others liquid and reported earlier [24, 26, 46, 47]. Verhejen et al [26] suggested that the saturation of contact angle occurs when charges accumulate in dielectric layer causing formation of shield and apparently further

change in contact angle is not possible. The earlier saturation of 1M NaCl solution is likely due to availability of more ions as compared to other liquid.

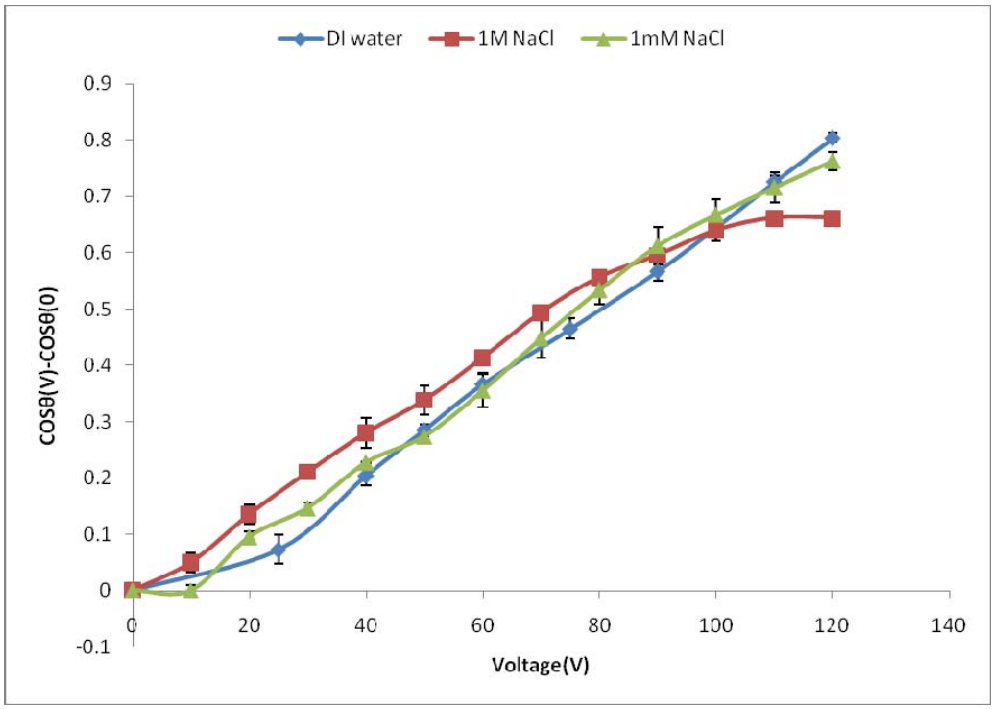

Figure 14 Contact Angle Measurements for Different Liquid on a Substrate having Dielectric Thickness of 2.05 µm

4.2.2 Reversibility of Electrowetting

The electrowetting is expected to be a reversible phenomenon. However, many researchers reported the irreversibility of electrowetting processes [26, 29, 34, 48]. The reversible nature of electrowetting was investigated by measuring the contact angle of different liquids for increasing and decreasing voltages. Figure 15, Figure 16 and Figure 17 show the contact angle measurements when voltage was ramped up and down in steps. DC voltage was used for the testing. The maximum voltage is 120V for measuring the contact angle changes. Then, voltage was lowered in steps and contact angle was measured until the voltage is lowered to 0V. The hysteresis of DI water droplet is smaller than the salt solution. In the beginning (when voltage was zero) and end of the test (when

voltage is made zero after ramping down) the contact angle values changes by 6° and 2° for salt solution (both 1mM NaCl and 1M NaCl) and DI water respectively. The irreversibility of electrowetting is attributed to the trapped charges. The trapping of charge in dielectric layer is more in aqueous droplet Also the electrowetting is not perfectly reversible for DI water also which suggest that charges were trapped at end of test. The possibility of impure DI water use during experiment is very likely.

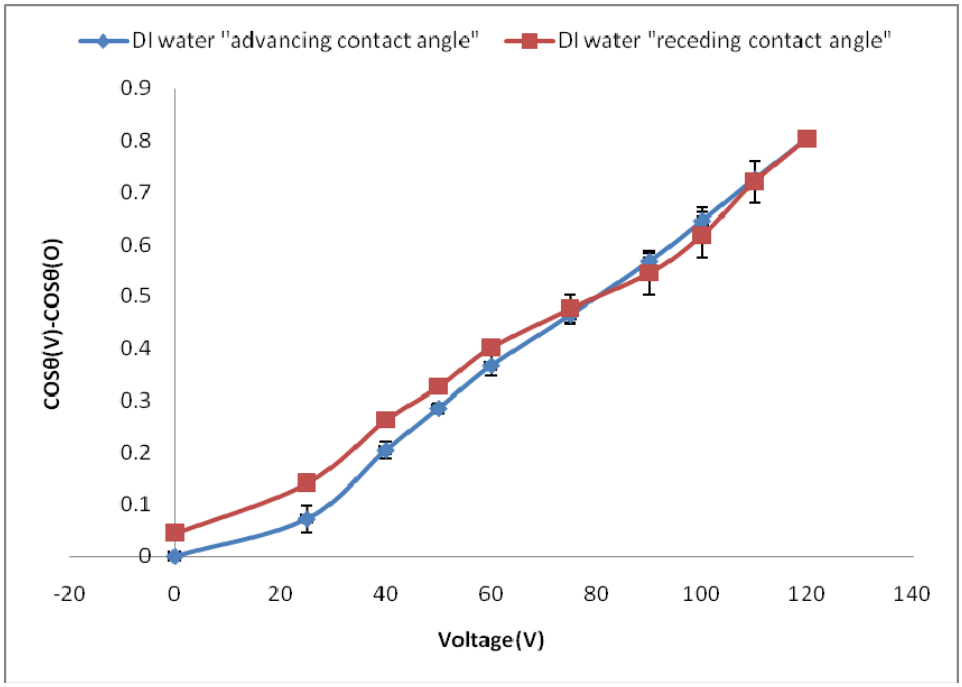

Figure 15 Reversibility of Electrowetting. Contact Angle Measurements for DI Water on Sample having Dielectric Thickness of 2.05 µm

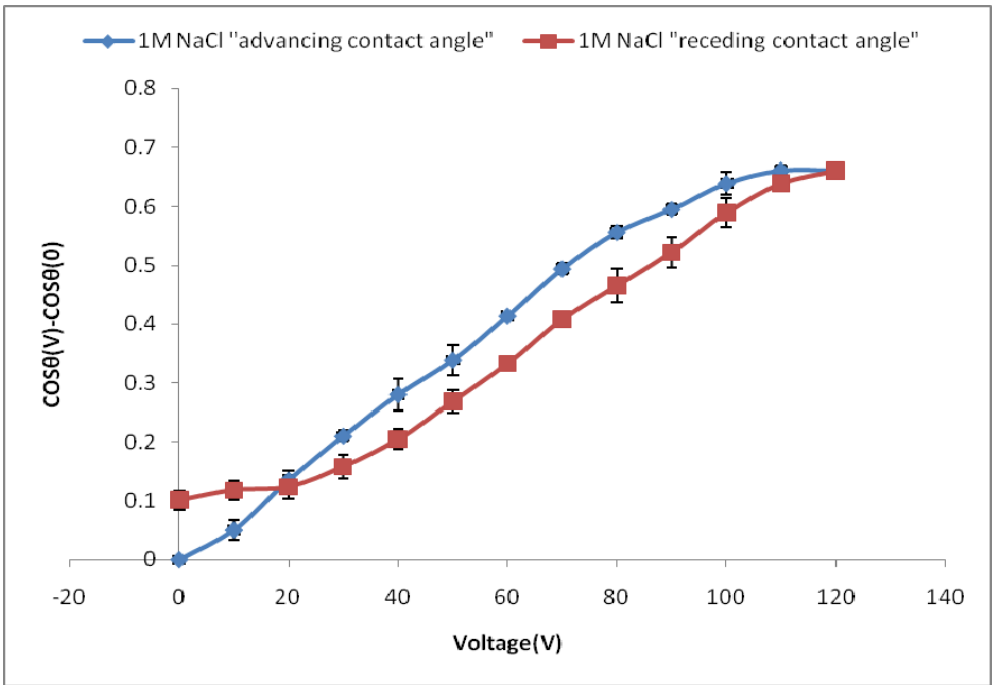

Figure 16 Reversibility of Electrowetting. Contact Angle Measurements for 1M NaCl Solution Sample having Dielectric Thickness of 2.05 µm

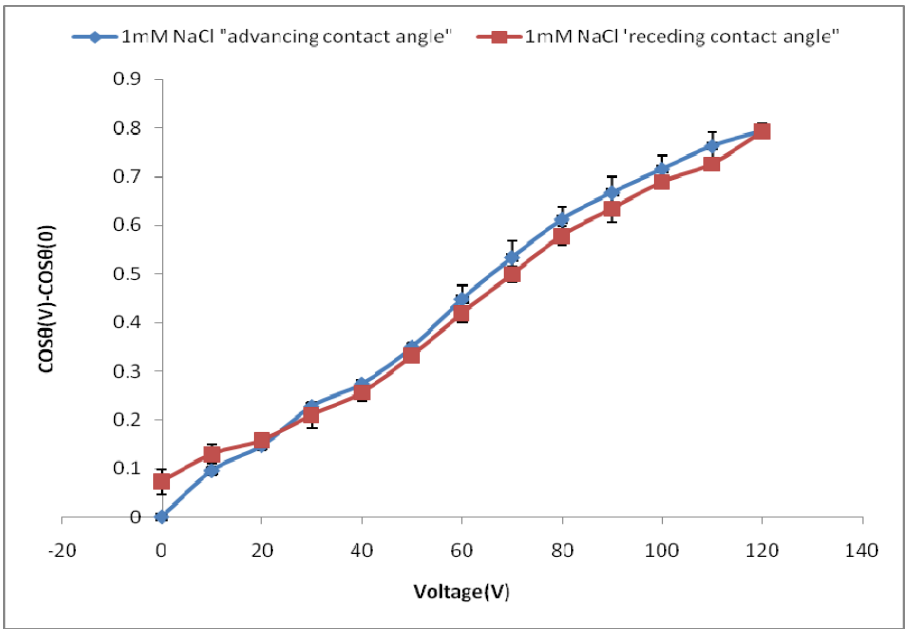

Figure 17 Reversibility of Electrowetting. Contact Angle Measurements for 1mM NaCl Solution Sample having Dielectric Thickness of 2.05 µm

4.2.3 Polarity Dependence

The electrowetting experiment is often done in two ways: applying the voltage across electrode and droplet by immersing wire electrode in liquid droplet and secondly by applying voltage across coplanar electrode and droplet is positioned between electrodes. The polarity of electrodes during electrowetting has been reported earlier [34, 49, 50]. Shih et al used the polarity dependency of electrowetting for pumping the liquid droplet. The authors named the polarity dependence phenomena *'Asymmetric Electrowetting on Dielectric (AEWOD)'*.

The polarity dependency of electrowetting has been investigated by measuring the contact angle for two possible experiment set up in this work. First, the droplet is grounded and second, the substrate (aluminum electrode) is grounded. The contact angle is measured for different voltage in both configurations.

Figure 18 , Figure 19 and Figure 20 show the contact angle measured for both above mentioned configuration for DI water, 1mM NaCl and 1M NaCl. The contact angle modulation for all liquids was lower when the aluminum electrode was grounded. Also the trend of contact angle change is found to be irregular in the aluminum grounded case as compared to the grounded droplet configuration. However, the dependency of polarity found to be more in 1mM NaCl compare to 1M NaCl liquid. This observation is inconsistent with the observed contact angle changes in earlier case. Perhaps, this irregular trend may be due to the imperfect surface morphology of substrate.

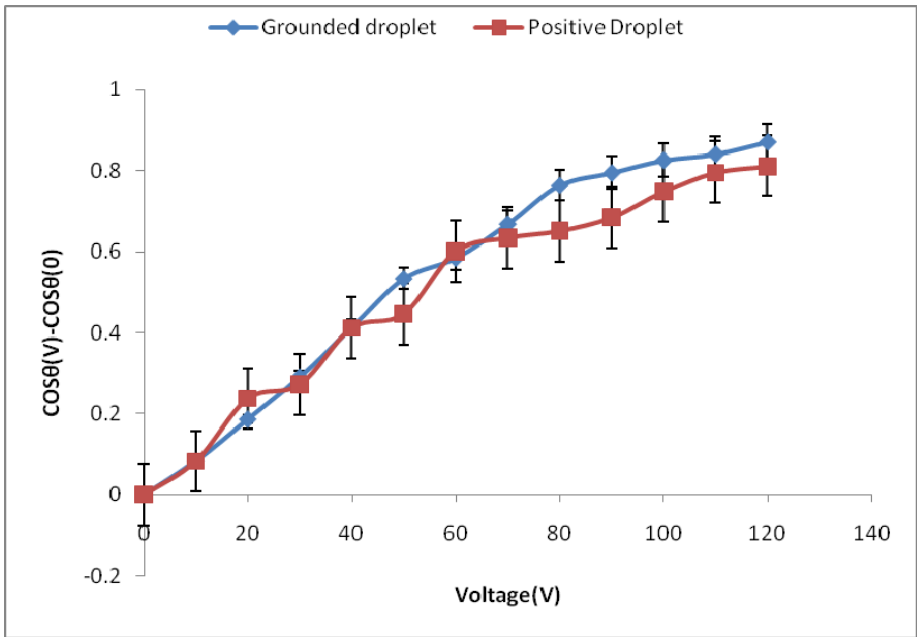

Figure 18 Asymmetric Electrowetting: Polarity Dependence of Electrowetting for DI Water on a Sample having Dielectric Thickness of 1.78 µm.

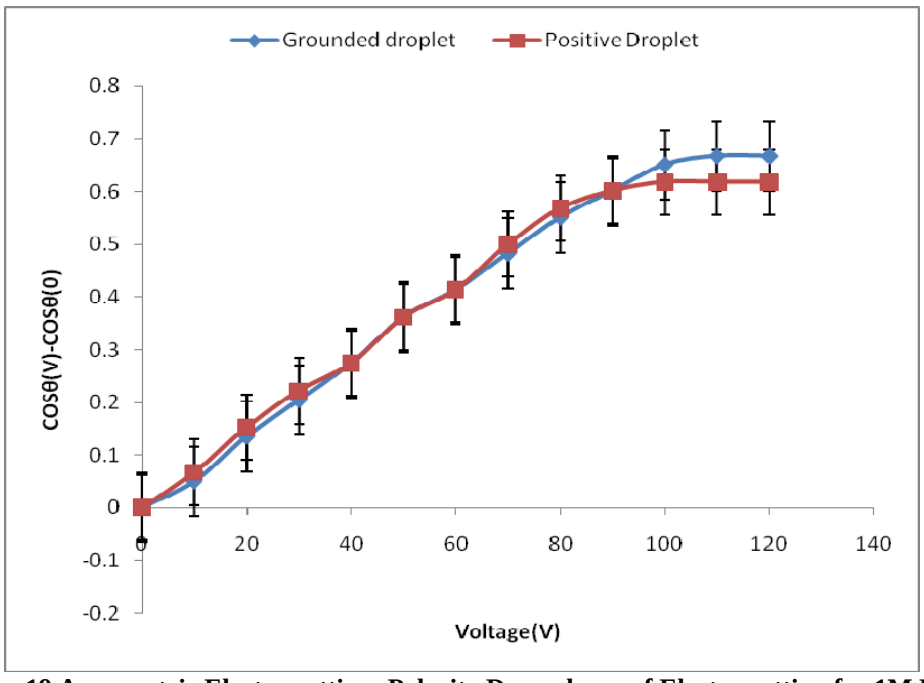

Figure 19 Asymmetric Electrowetting: Polarity Dependence of Electrowetting for 1M NaCl Solution on a Sample having Dielectric Thickness of 2.05 µm

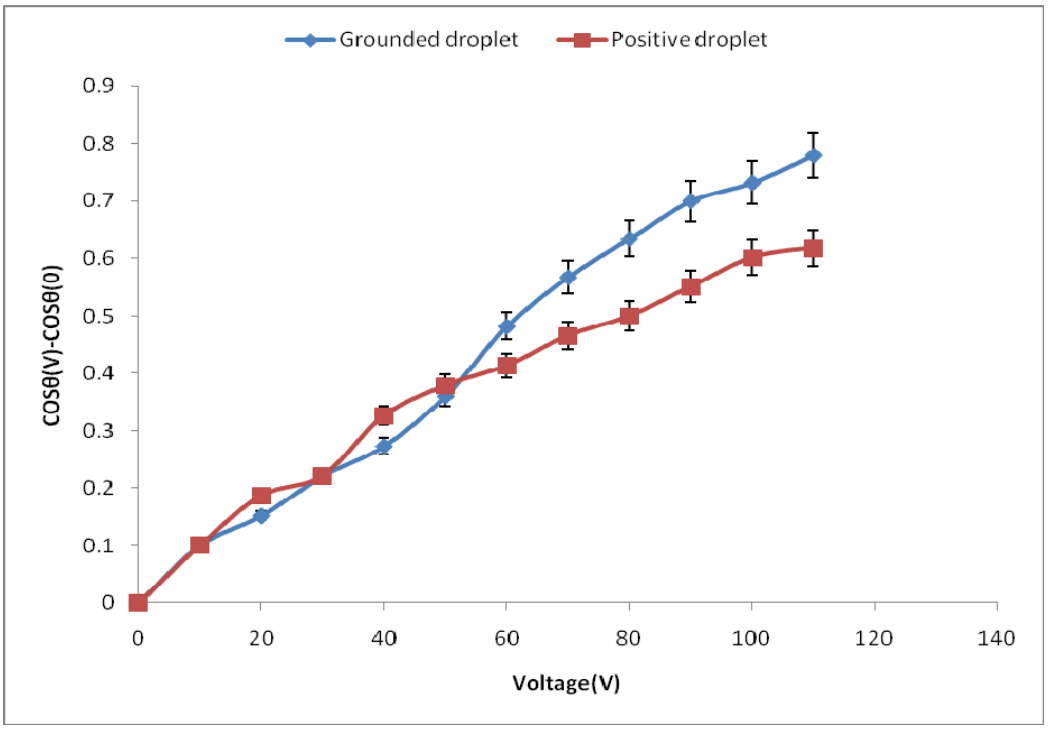

Figure 20 Asymmetric Electrowetting: Polarity Dependence of Electrowetting for 1mM NaCl Solution on a Sample having Dielectric Thickness of 2.05 µm

4.3 Electrowetting Force (EWF) Measurement

4.3.1 Predicted EWF

The electrowetting force was measured using nano indenter. The theoretical model and experimental procedures are discussed in a previous chapter. The analytical relations for EWF are expressed as equation 6.

Figure 21 shows the predicted EWF for perfect dielectric layer and floating droplet electrowetting configuration. Figure 22 compares the predicted EWF and measured EWF for different liquids at various voltages. The deviation of measured EWF at higher voltages from the predicted EWF attributed to the saturation of electrowetting phenomena at higher voltages.

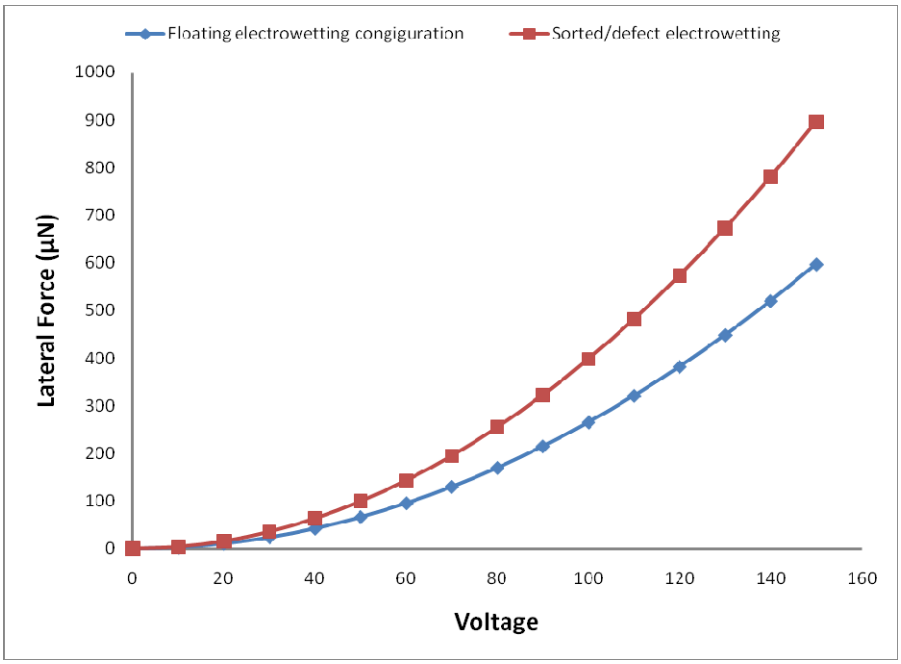

Figure 21 Electrowetting Force (EWF) Prediction for Floating Drop on Coplanar Electrode and Sorted or Electrode Coated with Defect on Dielectric Layer.

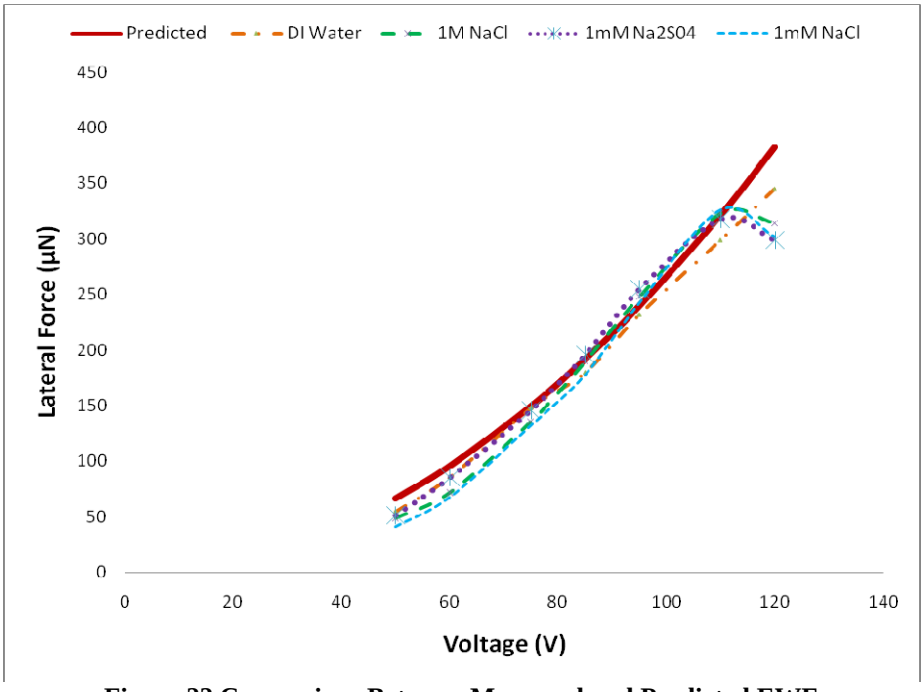

Figure 22 Comparison Between Measured and Predicted EWF

4.4 Measured EWF

Figure 23 shows the measured EWF for 1mM NaCl solution. The 75 V dc voltage was applied for 20 seconds. The electrode, in which the droplet was positioned at 3mm offset from the center of coplanar electrode gap, was grounded.

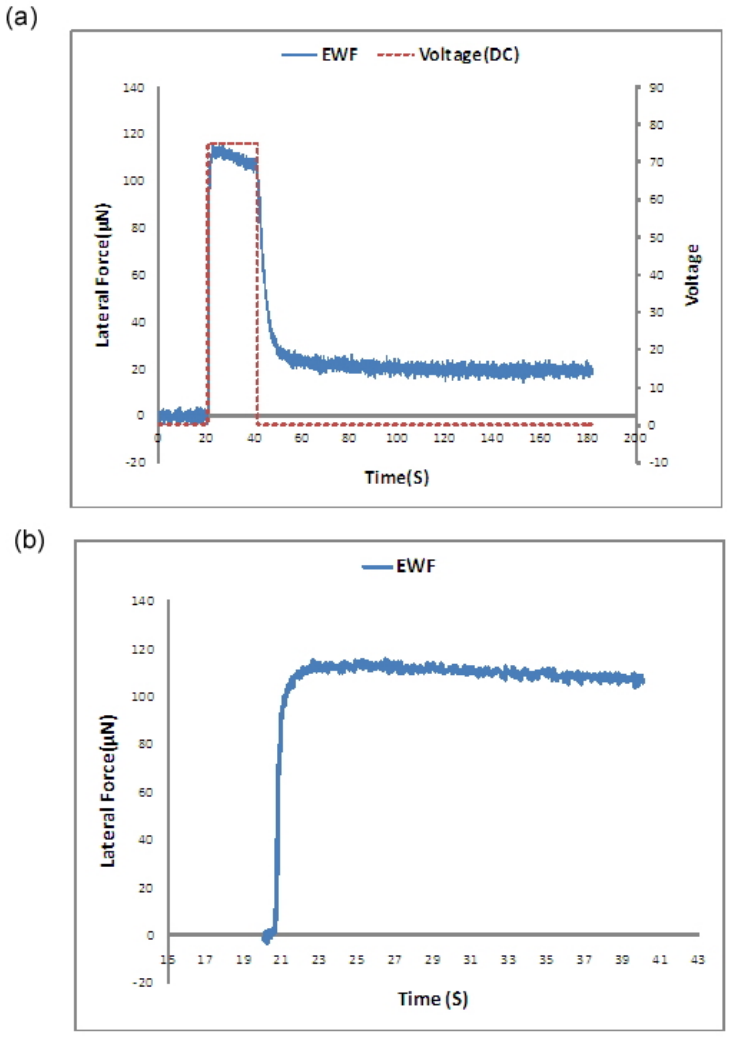

Figure 23 Measured Electrowetting Force for 1mM NaCl Solution. 75 DC Voltage Applied during time 20 to 40 second. Experimental Parameters: Droplet size = 55μL; the Offset Side of Electrode Grounded, Offset = 3mm (b) EWF during Voltage Applied Period.

The EWF peaks at the value of 114μN for 75 V DC voltages. The force measured during voltage applied period is shown in Figure 23 (b). Interestingly, the EWF decreases during the period of voltage applied. The force decreases by 8μN. The decrease in force during voltage applied period shows a decay phenomenon of the system. The change in force indicates that movement of droplet towards the electrode having low voltage strongly depends on the system performance. Also measured force shows that at the end of voltage, the system force never reaches its initial value. This was observed in every experiment.

The residual force value for 1mM NaCl droplet measured to be in the range of 20-35μN. Verheijen et al. [26] experimentally measured the contact angle of an electrowetting system and proposed that trapped charges may account for contact angle hysteresis. The change in contact angle during electrowetting system strongly depends on the trapped charges. The residual EWF after the voltage applied is related to the trapped charges in the system.

The series of experiments were carried out on different liquid to investigate the performance of electrowetting system for increasing applied voltage across the electrodes. The dc voltage pulses were increased manually. Figure 24, Figure 25, Figure 26 and Figure 27 show the performance of 1mM NaCl, 1M NaCl, DI water and 1mM Na_2SO_4 droplets respectively when the voltage across the electrodes was increased.

The contact angle saturation phenomena in electrowetting system have been reported by many researchers [11, 23, 24, 31]. The contact angle saturation is also observed in contact angle measurement in this work. The measurement of EWF at higher voltages evidently shows saturation phenomena in electrowetting system.

In contact angle measurement, after saturation voltage the contact angle is not changing. However, the saturation of electrowetting effect could be better explored using EWF measurement In EWF measurement method, the EWF increases with the voltage increase until the threshold value. After the threshold voltage the EWF decreases with increase in voltage. The value of threshold voltage is different for different liquids. The apparent decrease in force at higher voltages clearly indicates that performance of the electrowetting system diminishes after the threshold voltage.

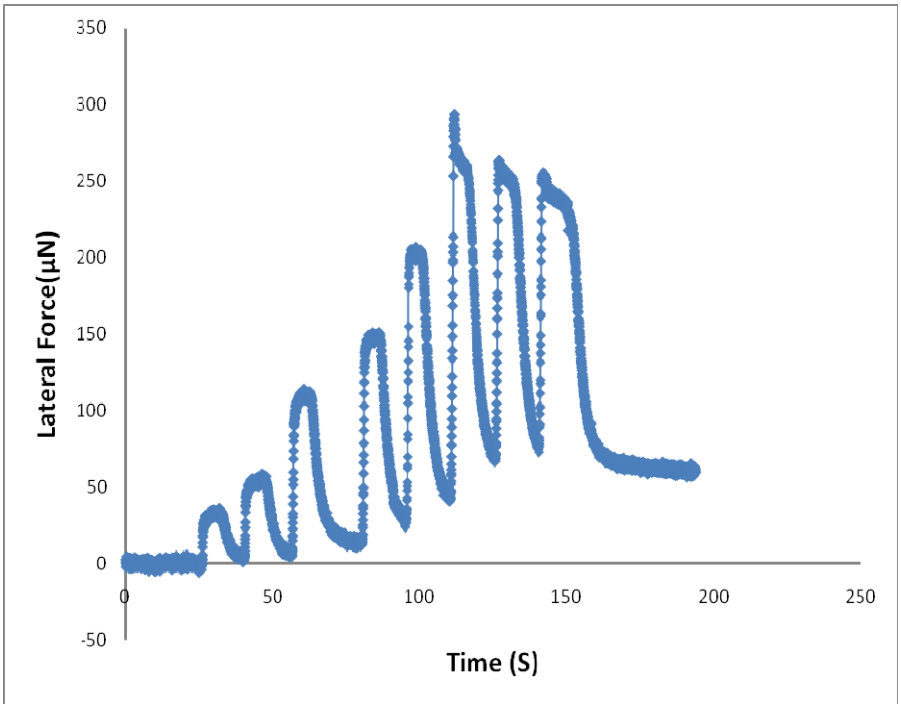

Figure 24 Electrowetting Force for 1 mM NaCl Solution. DC Voltage Ramped up. The Voltage Applied : 25V, 50V, 60V, 75V, 90V, 110V, 120V, 130V.

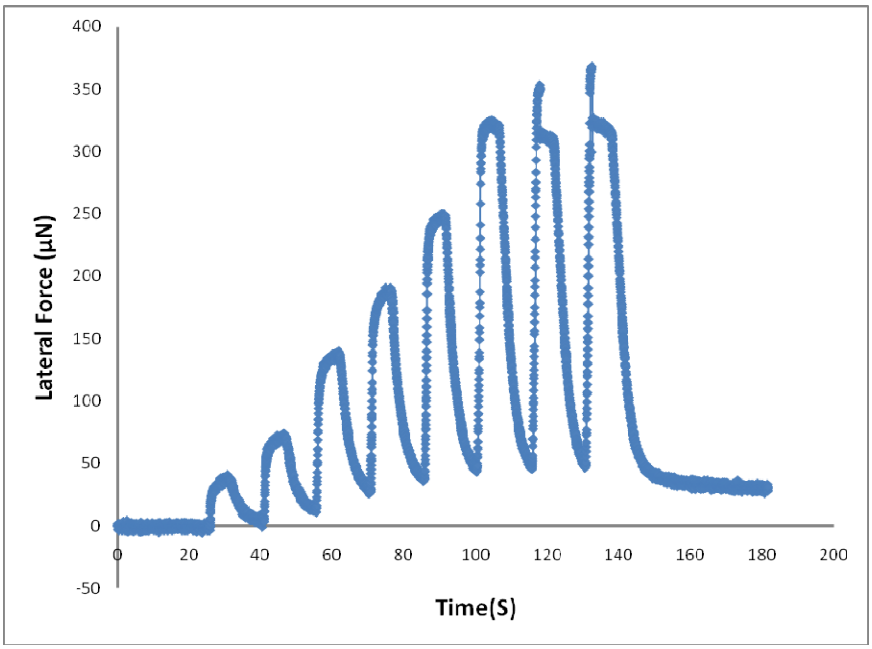

Figure 25 Electrowetting Force for 1M NaCl Solution. DC Voltage Ramped up. The Voltage Applied : 25V, 50V, 60V, 75V, 90V, 110V, 120V, 130V.

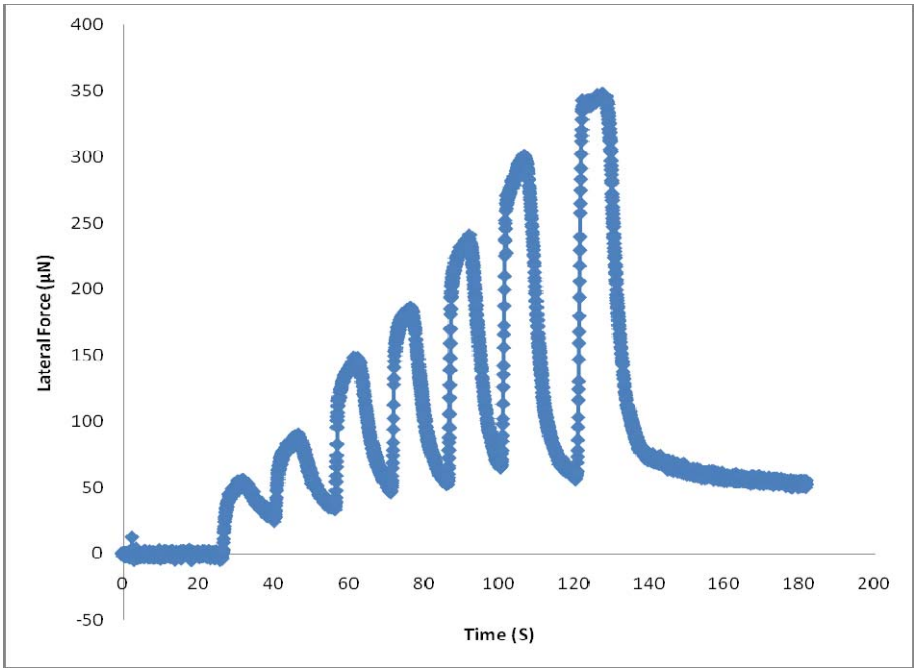

Figure 26 EWF for DI Water. DC Voltage Ramped up. The Voltage Applied : 25V, 50V, 60V, 75V, 90V, 110V, 120V, 130V.

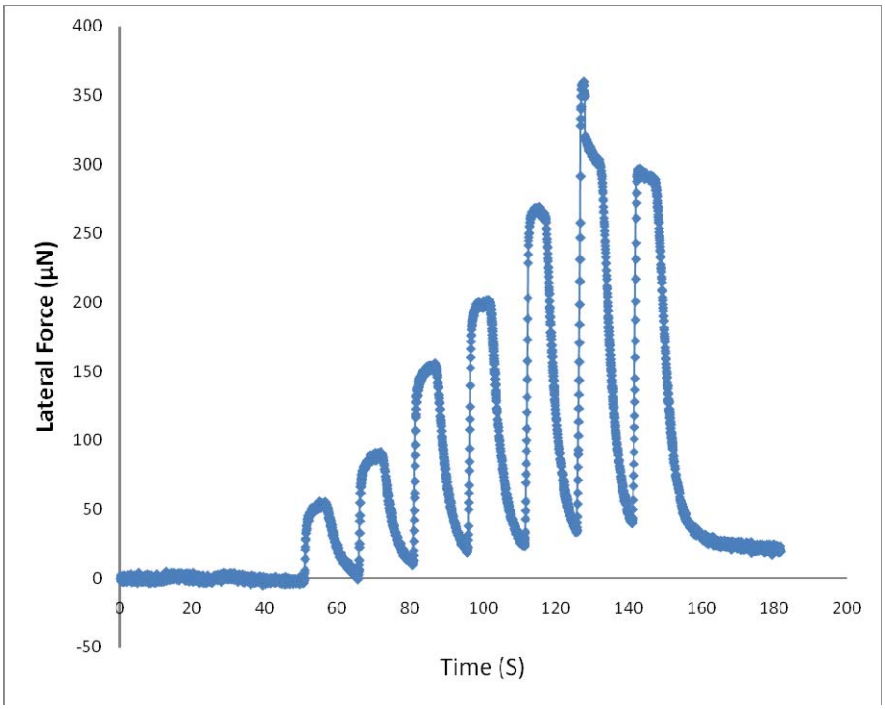

Figure 27 Electrowetting Force for 1mM Na2So4 Solution. DC Voltage Ramp-up. The Voltage Applied : 25V, 50V, 60V, 75V, 90v, 110V, 120V, 130V.

Additionally, the performance of aqueous solutions and DI water is clearly different at higher voltages. For aqueous solutions, the EWF measurement at higher voltages shows spikes while for DI water no spikes are observed. The spiky nature of EWF indicates that electrowetting system is unstable. The possible mechanism of spiky nature in aqueous solution can be better described in terms of charge injection at higher voltages. In electrowetting the change in contact angle (in this work EWF) with increasing voltage has two essential assumptions: first the liquid is conductor and second the dielectric layer is a perfect insulator. At higher voltages the possibility of violation of any one or both of these assumptions are fairy possible. The dielectric coating in this work is characterized for 75V dc. At higher voltages, the leakage current in these dielectric starts which violates the perfectly insulating coating assumption of electrowetting theory. In such cases, charges can be trapped inside the dielectric layer.

These trapped charges will decrease the effective voltage across the capacitor. Verhijin et al. [26] proposed a modified Young-Lipmann equation incorporating the affect of trapped charges. The modified mathematical relation is:

$$\cos\theta_1 = \cos\theta_o + \frac{\varepsilon_o \varepsilon_r (V - V_T)^2}{2\gamma_{lv}\delta}$$

Equation 12. Modified Young-Lipmann equation by Verhijin et al.

where V_T is the potential drop across capacitor due to trapped charges. The decrease in voltage across the capacitor will lead to decrease in EWF. However, the spikes observed in only aqueous solution case strongly suggest that there is a significance difference in trap charge mechanism between aqueous solution and DI water. In aqueous solution, the available ions in the liquid can aid the trap charge amount with the leakage current charge. In counterpart, for DI water case there is no available ions to be trapped inside the dielectric layer. The greater amount of trapped charges will lead to a greatly strained dielectric matrix and system stability can be highly disoriented leading to spikes in EWF measurements.

In 1999, Vallet et al. [51] studied the contact angle saturation phenomena experimentally using optical observations. For the aqueous solutions, the authors observe that droplet luminesces at high voltages. They observed the light emitting at short pulses with duration of 100 ns. After correlating the light emission and current measured at the same time in system, authors found that during the light emission time the current value spikes indicating the discrete discharging event. For low conducting fluid, like DI water authors observed a different phenomenon at higher voltages. Authors claim that during high applied voltage, small satellite droplets eject from the mother droplet in the case of

DI water. Interestingly, these high voltage events with liquid droplet in electrowetting found to be the same as for the saturation voltage.

During EWF measurements, the droplet is sandwiched between substrate and plate such that the entire plate is wetted. Given the very small dimension of plate and thickness of droplet after sandwiching, the possibility of small droplets is very unlikely. In EWF measurements, possibly this mechanism of spiking current after saturation voltage is similar to spiking of EWF values at higher voltages for aqueous solution. In case of DI water, the ejection of small droplets as suggested by Vallet et al. [51] at higher voltages is not possible during EWF measurement due to very restricted space for droplet ejection.

4.4.1 Polarity Dependence of Electrowetting System

The experiments are performed to investigate the affect of voltage polarity on EWF.

Figure 28 show the EWF measurements on 55µL 1mM NaCl droplet. The 75V dc voltage is applied across the electrode. At the beginning of the experiment (t=0 s), the electrode having the offset position of droplet was grounded. At time t=10 s, 75V DC voltage pulse was applied across the electrode. At t=30 s the voltage across electrode was made zero by turning off the voltage source output.

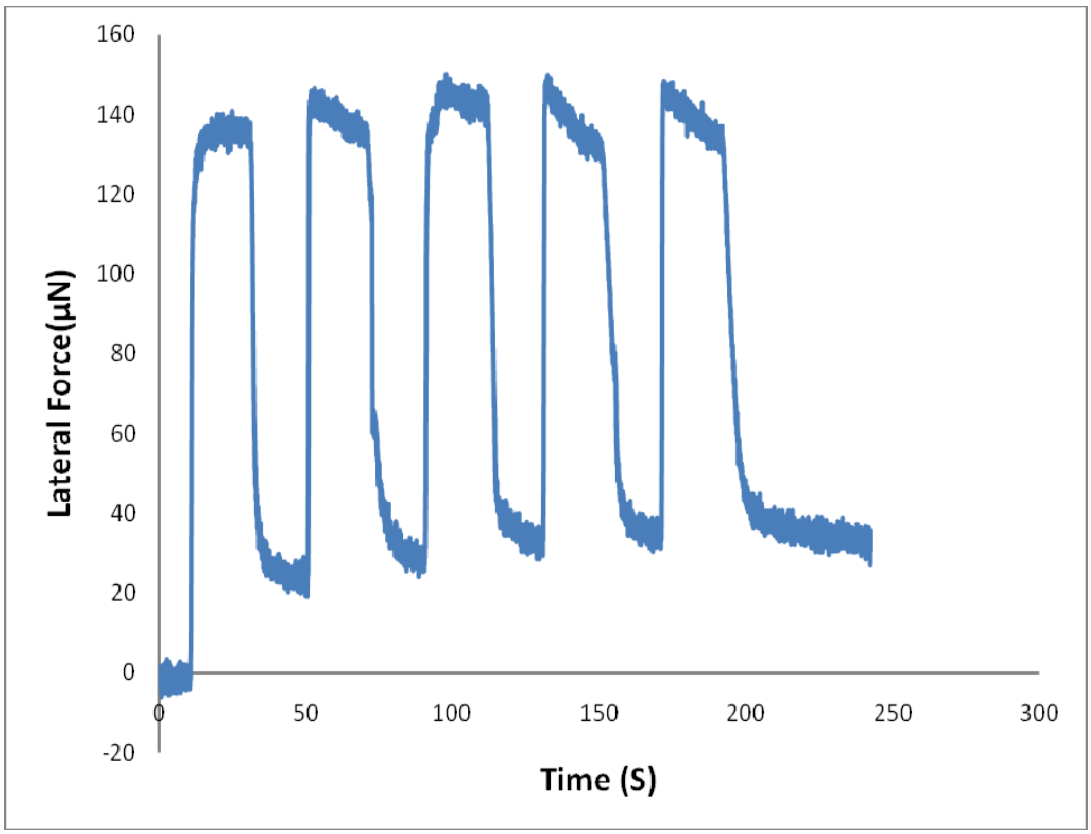

Figure 28 EWF for 1mMNaCl. 75V DC Pulse was Applied. The Electrode with Offset Droplet Position was Negative at the Beginning of the Test. During Second DC Pulse the Polarity was Reversed Making the Electrode with Offset Droplet as Positive and so on.

Then, the polarity of the electrode was changed manually. In all experiments the polarity of voltage across electrode changes likewise. The EWF measurement for 1mM NaCl indicates that the magnitude of EWF during any polarity combination is almost the same. However, the EWF during the voltage applied varies for different polarity. In the beginning (Figure 28), when the electrode having offset positioned droplet is grounded shows a small increase in EWF during the period of voltage applied. However, in the next dc pulse with opposite polarity, a steep decrease in EWF (from 144µN to 135 µN) can be observed. Later, in all dc pulses EWF is decreasing during the voltage applied. The decay in EWF after first dc pulse can be attributed to the charge trapped inside the

dielectric layer. Additionally, increase in residual force with every dc pulse is due to the charge trapping. At the end of the experiment the residual force is ~ 35μN.

Figure 29 shows the EWF for DI water with change in polarity for dc pulse. During the first dc pulse with the electrode, EWF increases during the voltage applied period like the 1mM NaCl droplet. However, the EWF observed to be almost constant for later pulses of dc voltage during voltage applied period. The amount of the residual force at the end of the experiment is ~ 25μN. The lesser amount of residual force for DI water as compared to 1mM NaCl drop is consistent with the theory of no available ions to be trapped inside the dielectric layer in DI water, opposite to 1mM NaCl case.

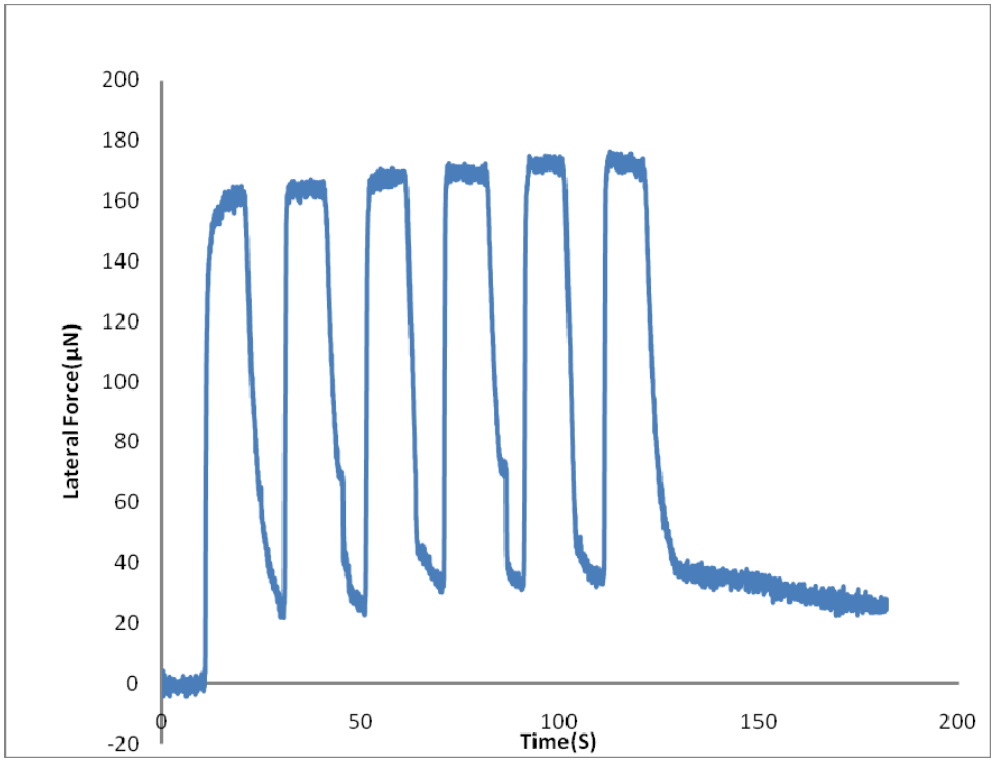

Figure 29 EWF for DI Water. 75V DC Pulse was Applied. The Electrode with Offset Droplet Position was Negative at the Beginning of the Test. During Second DC Pulse the Polarity was Reversed Making the Electrode with Offset Droplet as Positive and so on.

Figure 30 shows the EWF measurement for 1mM Na_2SO_4 droplet with change in polarity in applied dc pulse. The EWF measurement for 1mM Na_2SO_4 shows a spread

value. The EWF pick for different pulse is different. The one similarity with other liquid discussed (DI water and 1mM NaCl) is the increase in EWF during the first dc pulse. The scattered value in the EWF may be due to the substrate surface morphology. Also, the sample for this test had more than 24hr old dielectric coating. The possible adsorption of moisture from lab environment may have caused scattered EWF.

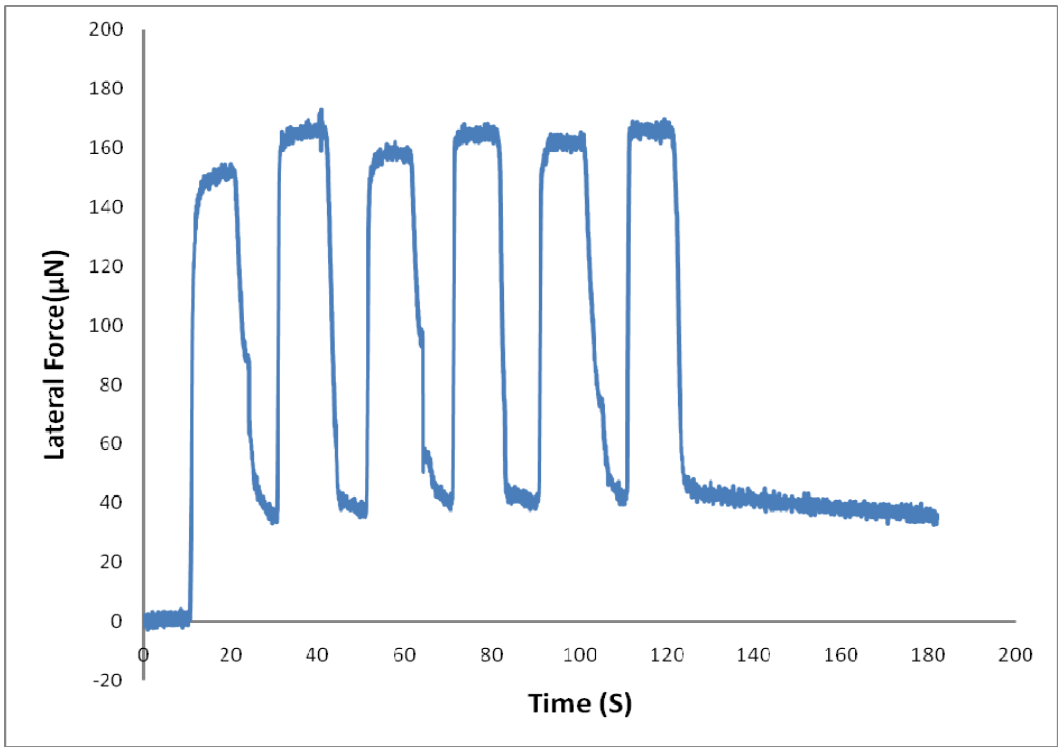

Figure 30 EWF for 1mM Na_2SO_4. 75V DC Pulse was Applied. The Electrode with Offset Droplet Position was Negative at the Beginning of the Test. During Second DC Pulse the Polarity was Reversed Making the Electrode with Offset Droplet as Positive and so on

4.5 Electrochemical Corrosion

The reliability of MEMS devices and packaging has been researched for more than one decade. The use of thin metallic film in micro devices has been well established. The very common metal used in micro devices is aluminum. Often, a thin film of dielectric layer is coated over the metal film to avoid the electrochemical corrosion. The failure of dielectric layer, either from defect or voltage breakdown, can initiate corrosion

of metal film. The reliability of micro devices with respect to corrosion has been researched by many [52-55].

The thin dielectric film coated metal electrode is generally used in electrowetting with aqueous solution as liquid droplet Also the demand of low voltage electrowetting claims the use of very thin film of dielectric layer. Given the small dimension of electrode, makes the electrowetting system very prone to electrochemical corrosion. Recently, Nanayakkar et al [56] explored the use of ionic fluid instead of aqueous solution in electrowetting systems.

In this work, the electrochemical corrosion has been observed during EWF measurement of electrowetting system. In electrowetting system the electrochemical corrosion is initiated by the failure of dielectric layer. The failure of dielectric can occur either due to voltage breakdown or exposure of defects on dielectric to electric field. Often it is a combination of factors since dielectric breakdown typically occurs in the vicinity of defects.

Figure 31,Figure 33 and Figure 38 show the EWF measurement where defects were observed after testing. In all cases 75 V dc pulse with change in polarity has been used to measure the EWF. Figure 31 show the EWF measurement for 1mM NaCl solution. When first 75V dc pulse is applied to the system, the measured EWF is similar to the other cases discussed. During first dc pulse, the electrode having offset droplet position was grounded. When the voltage polarity was reversed, the force sign changes which should not be observed according to equation 4. This can be discussed in terms of electrochemical corrosion theory. When the electrode having offset droplet position is grounded, it behaves like an anode. When the voltage across the electrodes is applied, the

droplet tends to move to the small area electrode. Droplet movement should be in the same direction also, when the voltage polarity is changed. However, when the voltage polarity is reversed, the force sign changes indicating the change in nature of the droplet motion. This opposite nature of motion of liquid is only possible if the large area electrode has the larger voltage across it. This could occur if the small area electrode was degraded.

In this work, aluminum has been used as the electrode material. Aluminum is a very reactive material and forms oxide very quickly once exposed to water or air. This suggests that when the voltage polarity changes, the electrode (now cathode) passivates. The passivity of aluminum is due to the formation of an oxide. The formation of passive layer has been observed after the testing by examining the test spot.

Figure 33 and Figure 38 show the case of 1mM NaCl and DI water droplet when the voltage polarity changes similar to earlier discussed case. The spikes as in EWF measurements indicate the trapping of charges in dielectric layer leading to failure. The change in sign of the force has similar reason as discussed above. Figure 32 and Figure 34 show the damaged spot on the substrate due to electrochemical corrosion for EWF measurements corresponding to Figure 31 and Figure 33, respectively.

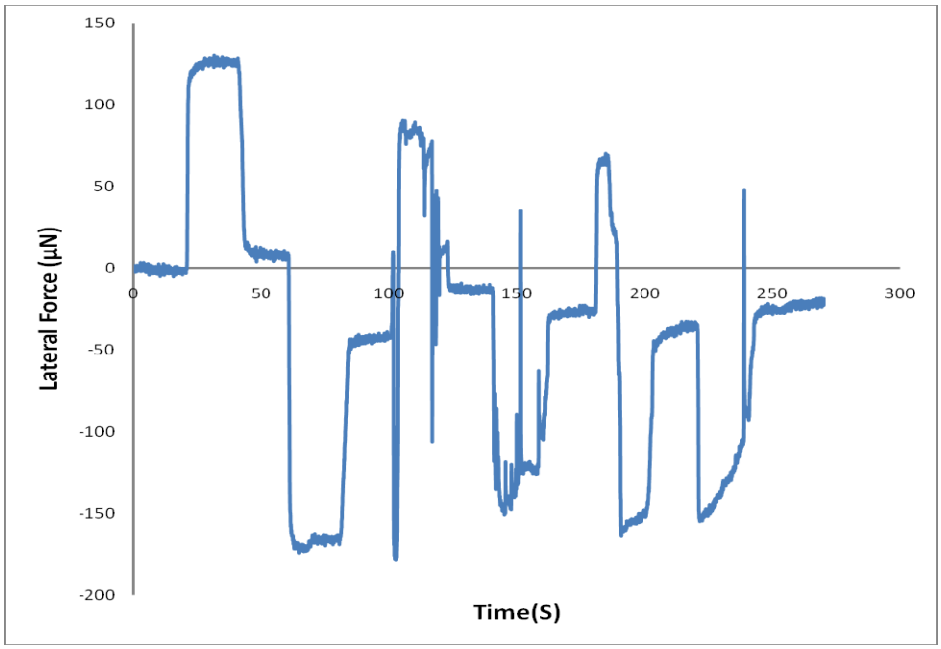

Figure 31 Electrochemical Corrosion: EWF Measurement at 75V DC Polarity Change for 1mM NaCl Droplet. Change in Sign of the Force and Spikes in EWF Spectrum Due to Electrochemical Corrosion.

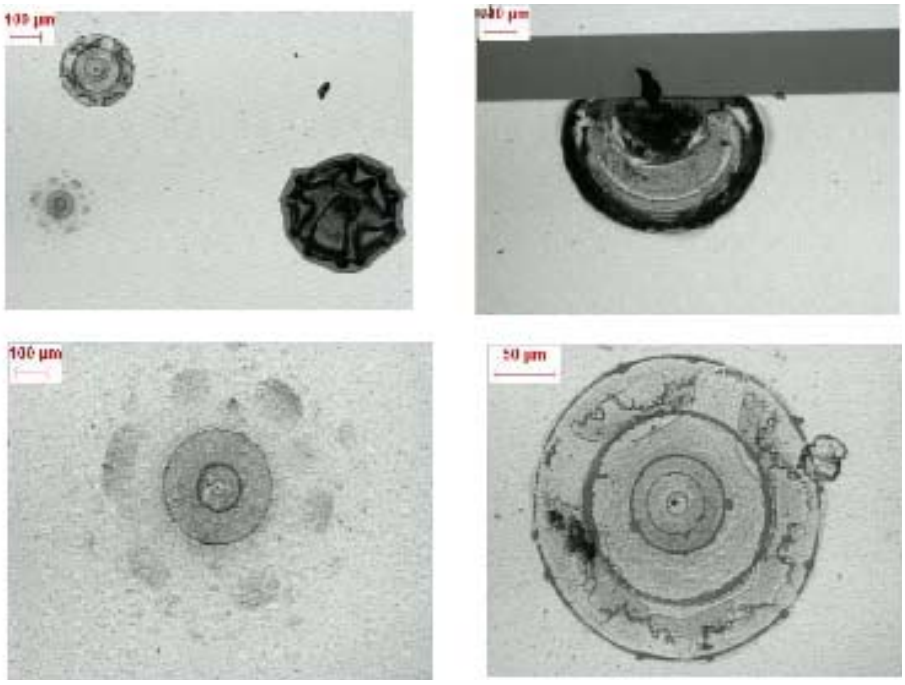

Figure 32 The Damaged Surface on Substrate due to Electrochemical Corrosion for EWF Measurement Corresponding to Data from Figure 31

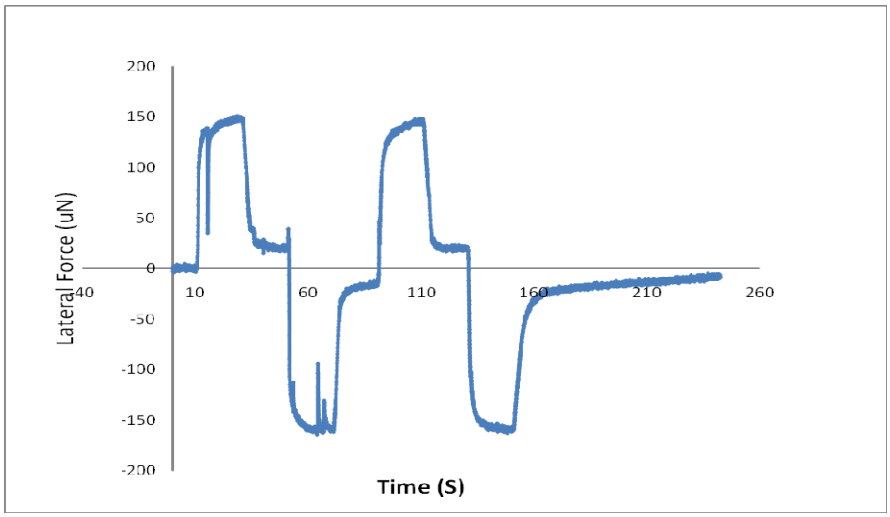

Figure 33 Electrochemical Corrosion: EWF Measurement at 75V DC Polarity Change for 1mM NaCl Droplet. Change in Sign of the Force and Spikes in EWF Spectrum Due to Electrochemical Corrosion.

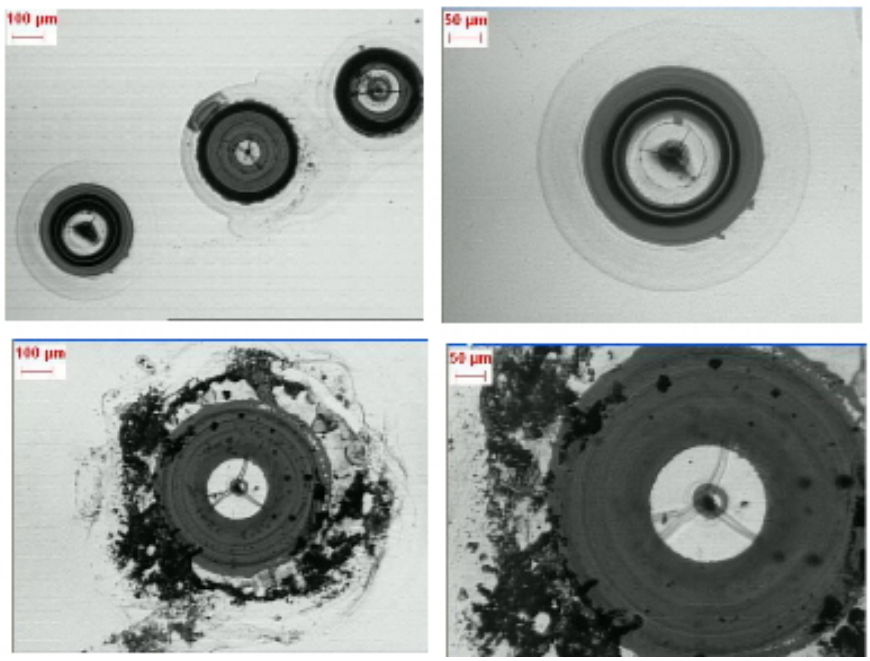

Figure 34 The Damaged Surface on Substrate due to Electrochemical Corrosion. The Damaged Surface on Substrate due to Electrochemical Corrosion for EWF Measurement Corresponding to Data from Figure 33

Figure 35 and Figure 36 show the scanning electron microscope (SEM) image of the damaged spot corresponding to EWF measurement Figure 33 for two different

magnifications. Figure 37 show the Energy Dispersive Spectroscopy (EDS) analysis of the corroded spot. The high presence of fluorine (F) in the EDS spectrum indicates the precipitation of fluorine from CYTOP™ after the electrochemical corrosion.

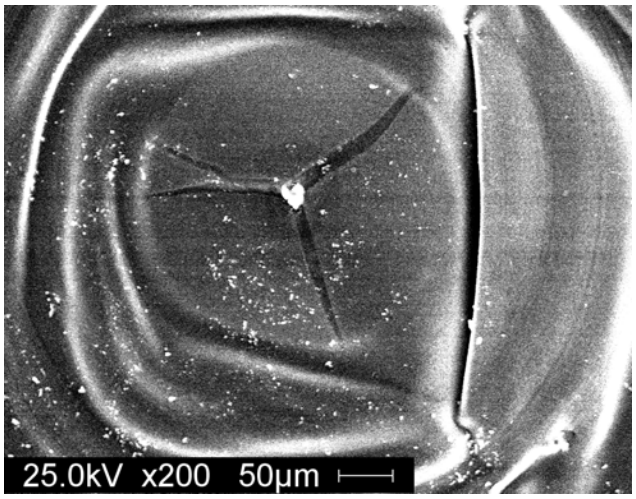

Figure 35 SEM Image of Damaged Test Spot Due to Electrochemical Corrosion. Magnification: x200

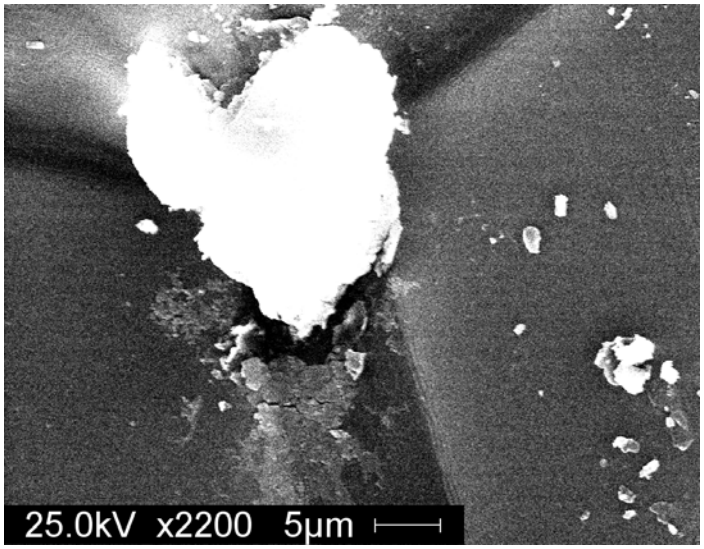

Figure 36 SEM Image of Damaged Test Spot due to Electrochemical Corrosion. Magnification: x2200

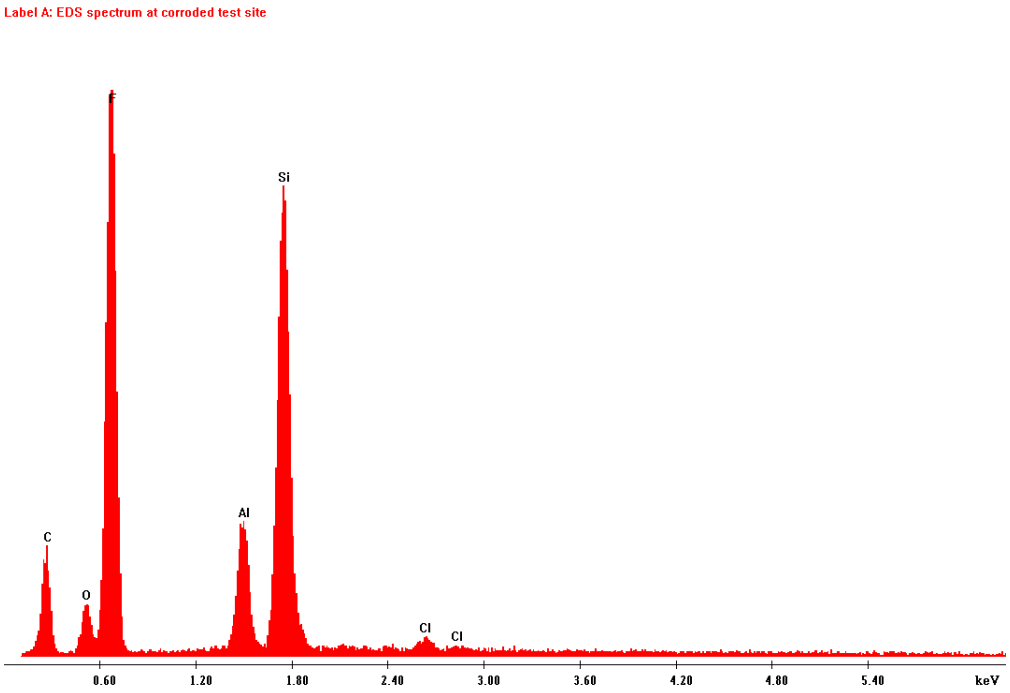

Figure 37 EDS Analysis of Damaged Test Spot.

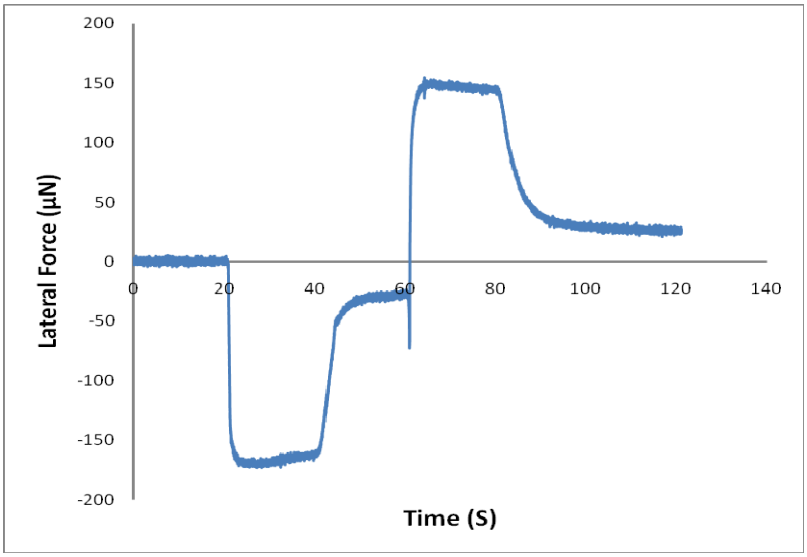

Figure 38 Electrochemical Corrosion: EWF Measurement at 75V DC Polarity Change for DI Water. Change in Sign of the Force and Spikes in EWF Spectrum due to Electrochemical Corrosion

The defects observed due to electrochemical corrosion are circular in shape, like doughnuts. When the dielectric layer fails, the electrons diffuse in the dielectric layer. The diffusion of electrons creates path for the flow of water molecule and oxygen which

forms oxide as soon as it comes in contact with aluminum film. The aluminum layer degrades by electrochemical reaction and possibly creates the pressure beneath the dielectric (CYTOP™) layer. Later, the delimitation of dielectric layer exposes the aluminum thin film and corrosion starts at the dielectric/aluminum interface.

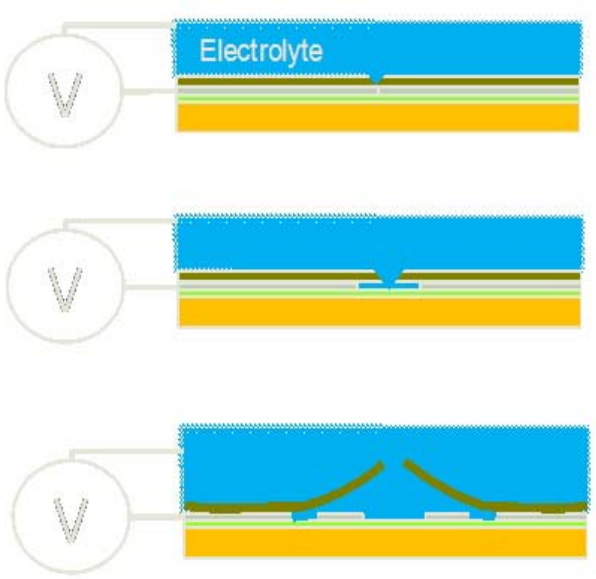

Figure 39 The Corrosion of Al Film and Delimitation of CYTOP™

CHAPTER 5 ENVIRONMENTAL EXPOSURE OF THE ELECTROWETTING SYSTEM

5.1 Introduction

In this chapter, the effect of environmental exposure on electrowetting system is studied. The changes in contact angle on a substrate with time immersed in liquid substrate have been carried out. In the second part of this chapter, the electrochemical impedance spectroscopy results are presented.

5.2 Contact Angle Measurement with Environmental Exposure

Electrowetting actuated devices are often exposed to the working liquid or other ambient environments. The performance of the electrowetting could degrade due to the environmental exposures. Electrowetting experiments are being conducted in air or liquid medium. Different types of Oil are the only medium reported so far as liquid medium. The use of olive oil and Fomblin vacuum oil is being reported in recent years [22, 23, 29], which reduces the contact angle hysteresis.

While air is often used in place of a oil as the environmental medium, the samples are also repeatedly exposed to aqueous drops that are manipulated via electrowetting. These drops often contain concentrations of various salts to improve conductivity. This work considers changes due to exposure to the aqueous fluids that are present in virtually all applications.

The substrates were immersed in a test fluid and removed at varying intervals of time for testing. After testing samples were immersed for additional exposure. The test substrate used in this experiment was processed similar to the contact angle measurement testing. Three types of immersion liquid were tested, DI water, 1mM NaCl and 1mM Na_2SO_4. The substrates were immersed in all liquids such that only the dielectric layer coated was in touch with the liquid. The test fluid is prevented from contacting the dielectric-free zones with exposed aluminum film area to overcome the possible corrosion of the bare metal. The contact angles were measured at regular intervals with voltage change to observe the effect of immersion on electrowetting performance. Figure 40, Figure 41, and Figure 42 show the contact angle measurement for 1mM NaCl, 1mMNa_2SO_4 and DI water respectively.

The contact angle for the substrate immersed in 1mM NaCl shows a significant change when the immersion time is 30 min. The contact angle at 75V for immersion time t=0 and t=30 min is almost the same as shown in Figure 40, but the difference in trend can be easily observed. The contact angle changes significantly after 2 hours of immersion time. Interestingly, the contact angle at zero voltage also decreases indicating the change in dielectric layer composition. The magnitude of change in the contact angle with a given applied voltage decreases as the immersion time increases. The same observation is made in the case of 1mM Na_2SO_4 (Figure 41) also. However, the change in contact angle with DI water as immersion liquid is minimal (Figure 42).

In the literature, the change in contact angle over time has been reported previously [57-61]. Lee et al. [57] reported the change in contact angle of different type

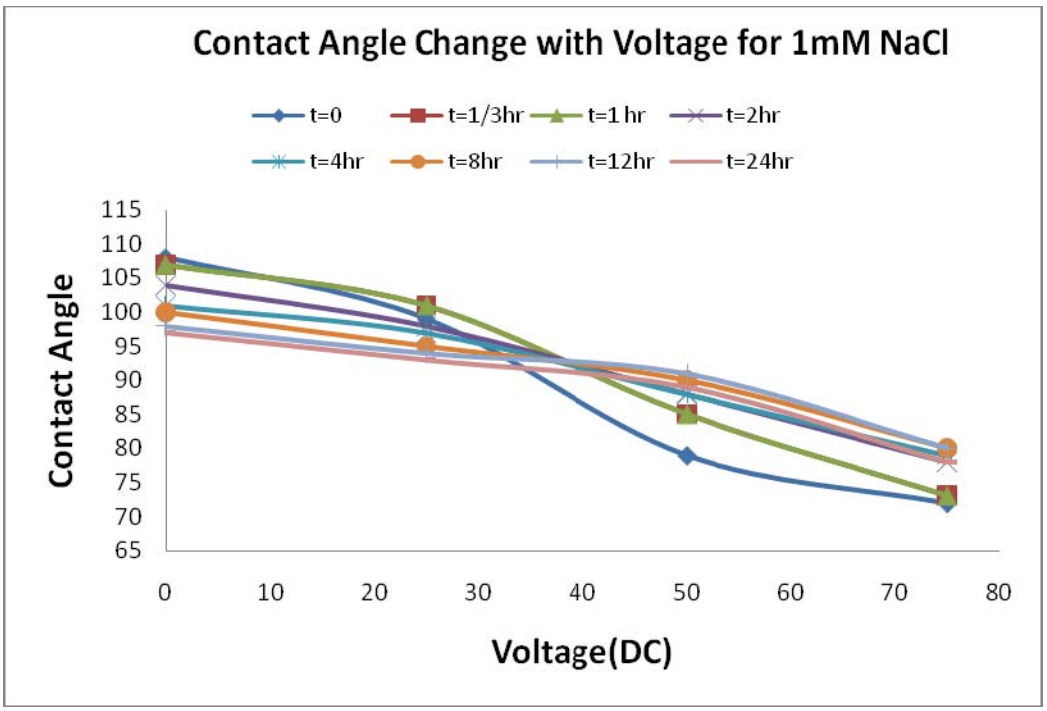

Figure 40 Change in Contact Angle for 1mM NaCl Droplet over Time

of liquids, polar, nonpolar liquids etc. on the fluropolymer over time. Authors claim that the decrease in contact angle over time is due to the interaction of ions with the polymer over time. Li et al [59] reported the change in contact angle of water droplet with time on the poly vinyl (PVC) membrane. Authors claimed that the penetration of water inside the membrane changes the membrane properties in terms of wettability. Interestingly, the change in contact angle is more for the first 2 hours and then become slower. The cross linking between ions in polymer after penetration changes the polymer's surface energy [59-61]. Wang et al. [58] experimentally measured the contact angle of water on polymer by sessile drop method. The droplet was kept on surface and contact angle was measured at regular time intervals. The time-dependence in contact angle measurement was mainly attributed to the surface reconstruction when water drops were deposited on polymer surfaces. The starting contact angle was contributed by the hydrophobic component on

polymer surface and the equilibrium contact angle mainly by the hydrophilic component of polymer.

The change in contact angle with liquid immersion for CYTOP™ has not been reported earlier. However, the mechanism of change in contact angle for other organic polymers will possibly be the same as the change in contact angle of CYTOP™ in this work.

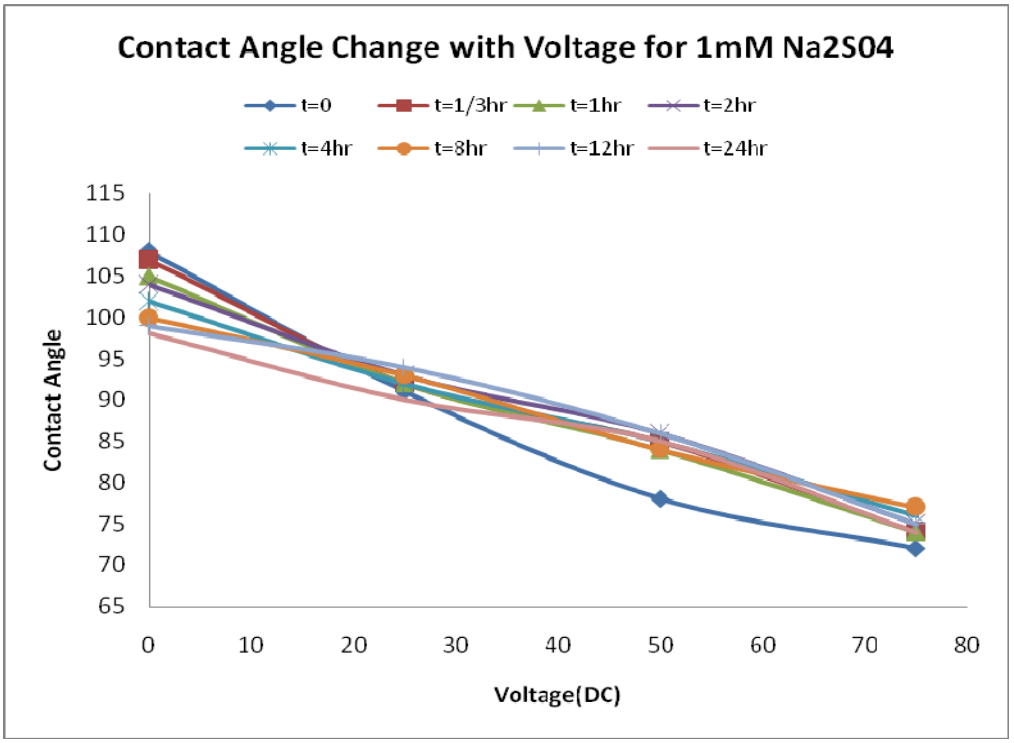

Figure 41 Change in Contact Angle for 1mM Na2SO4 with Immersion Time

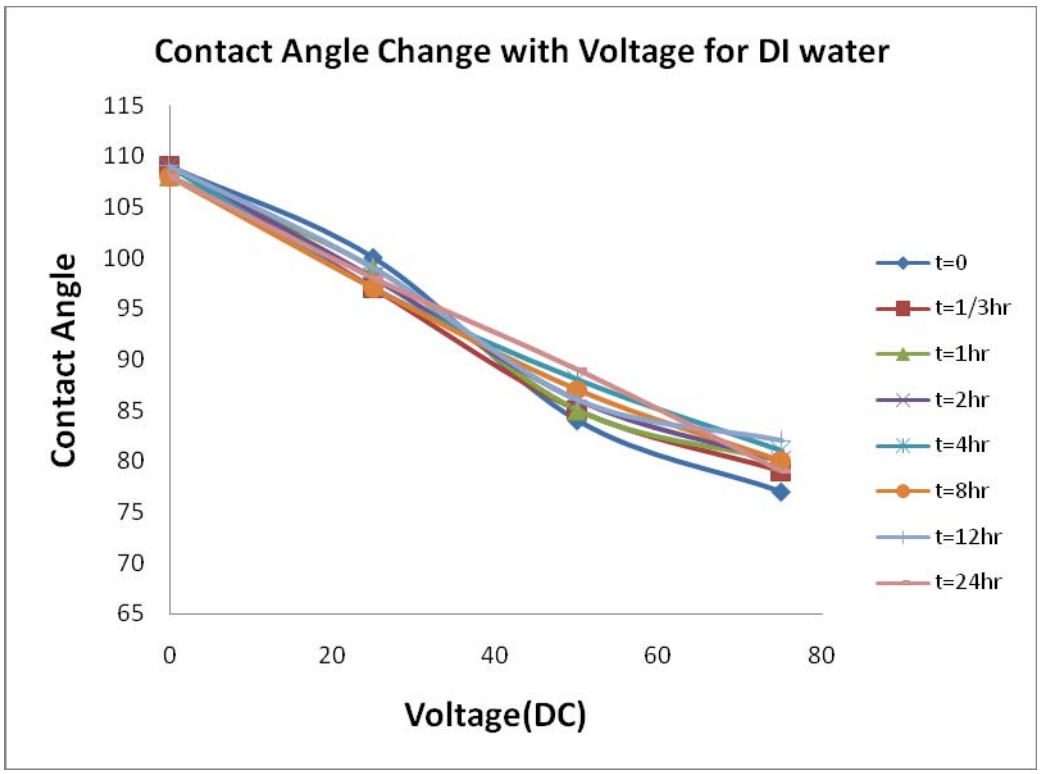

Figure 42 Change in Contact Angle for DI Water with Immersion Time

The change in contact angle is higher for 1mM NaCl as compared to the 1mM Na_2SO_4. The mechanism of the interaction of ions present in liquid and polymer can be attributed to the change in contact angle over time. Possibly the diffusion of ions into CYTOP™ layer is responsible for the change in contact angle with time. Additionally, diffusion of ions in the dielectric layer is also accountable for the poor electrowetting performance over time. Figure 43 show the time constant of contact angle decay for different liquid .The time constant for DI water, 1mM Na_2SO_4 and 1mM NaCl is found to be 0.20 hours, 0.90 hours and 1.20 hours.

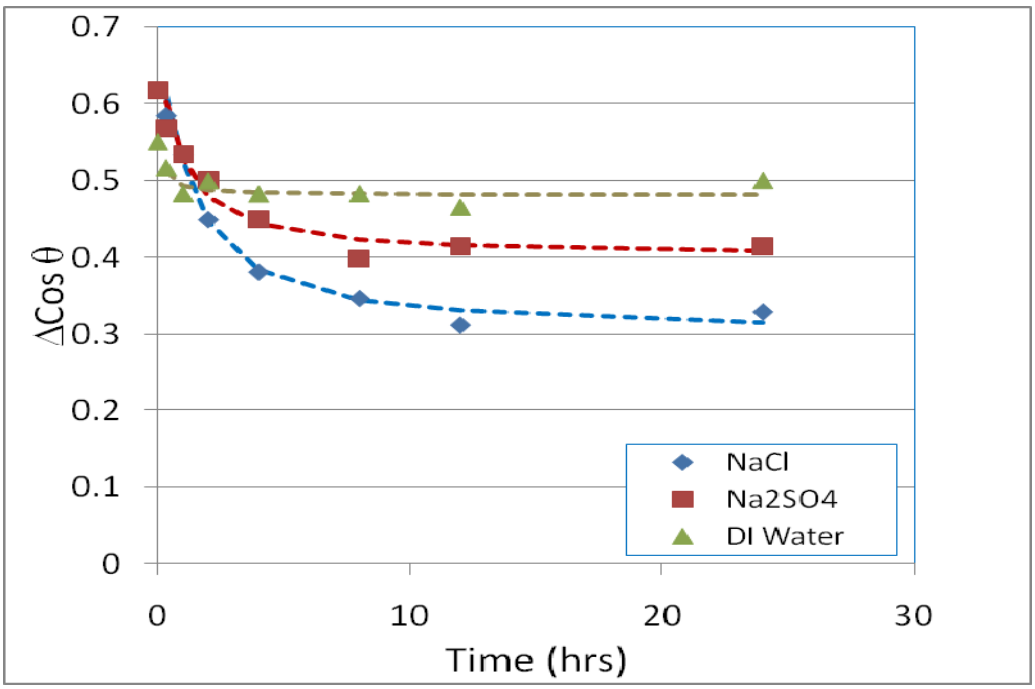

Figure 43 Time Constant of Steady Decay in Electrowetting Response due to Liquid Exposure

Figure 44 compares the contact angle modulation for a voltage change of 75 V for all three types of liquids. Clearly, the decrease in contact angle modulation for 1mM NaCl liquid is significant (from 34 to 20 degrees over 24 hrs).

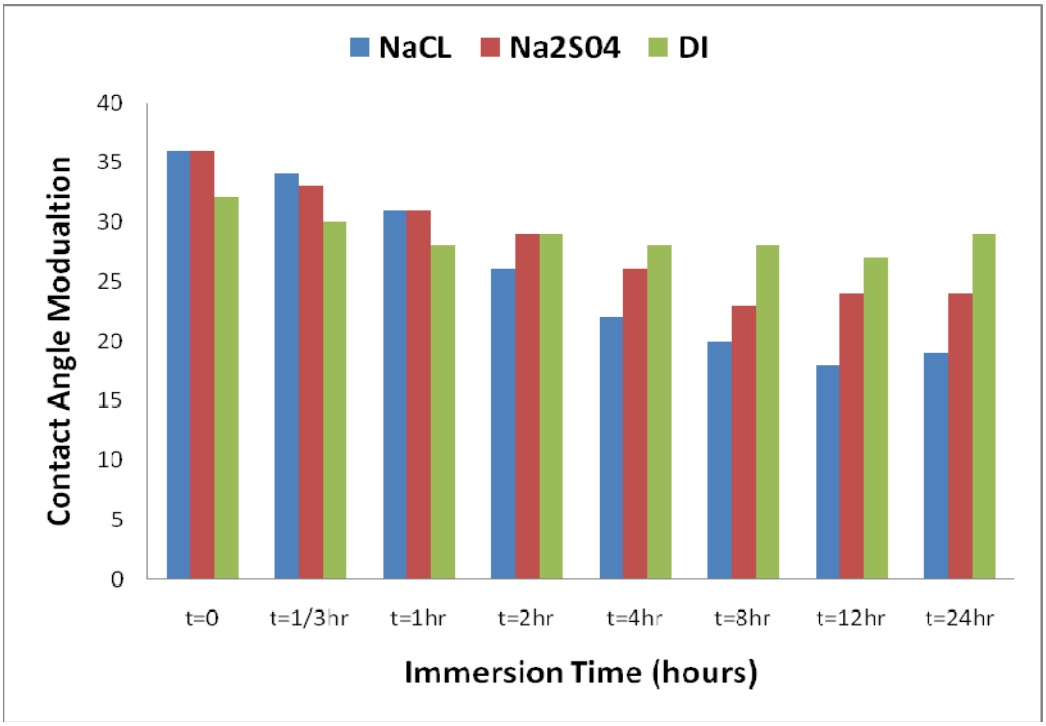

Figure 44 The Change in Contact Angle Modulation for Different Fluids with Immersion Time.

5.3 Electrochemical Impedance Spectroscopy

The electrochemical impedance measurement is carried out to investigate the change in capacitance of dielectric layer (CYTOP™) over time. Experiments were performed on the three different samples fabricated by the method discussed in chapter 3. The experimental parameters were kept identical for all three different samples. The experimental specifications were: maximum frequency of 100 KHz, minimum frequency of 1 Hz and 1 mV rms AC voltage. The electrolyte used in all experiment runs were 1mM NaCl solution. The experiment was performed for 4 hours to observe the change in capacitance. The data were collected over different periods of time after the electrolyte was poured into the cell. The sample specifications are listed in Table 1.

Table 1 Sample Specifications

Sample Number	Thickness (μm)
1	1.93
2	1.68
3	1.73

The percentage increase in the capacitance of the CYTOP™ thin film with immersion time is plotted in the Figure 45.

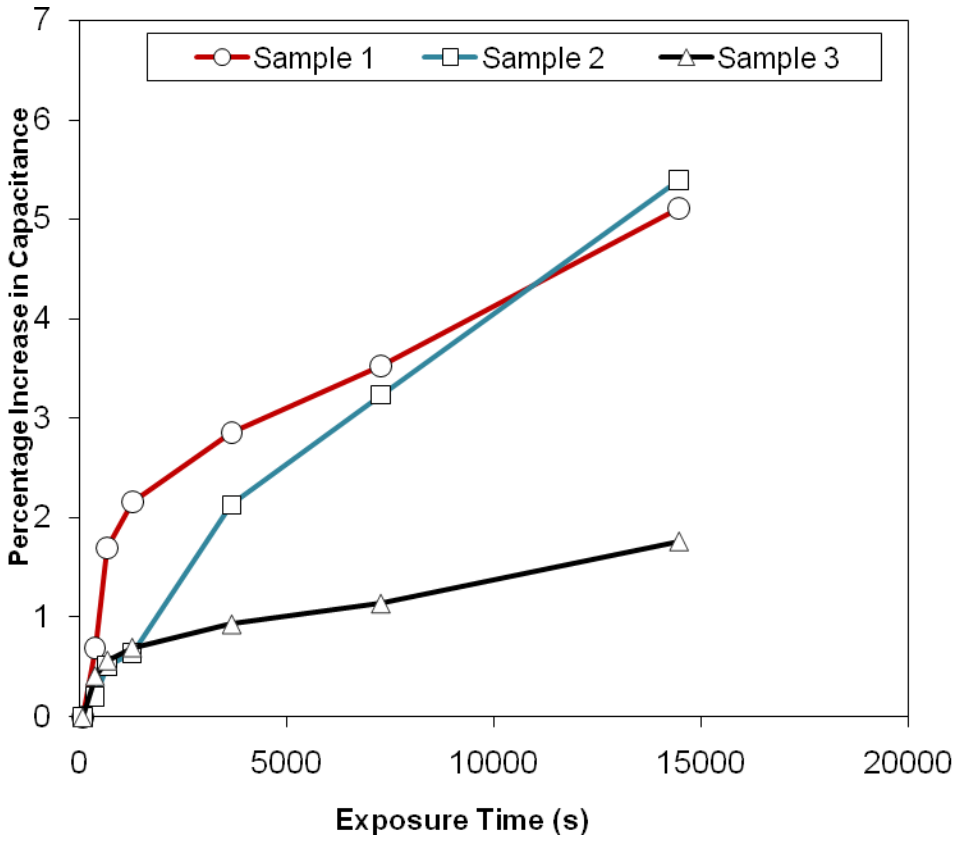

Figure 45 Percentage Increase in Capacitance with Exposure Time

The maximum increase (~5.40%) in the capacitance with immersion time of 4 hours was observed for the sample 2 with respect to the initial capacitance. The minimum

increase (1.77%) was observed for the sample 3. The marginal difference in enhancement of the capacitance between samples is possibly attributed to the moisture observation from lab air prior to experiment.

Figure 46 show the increase in capacitance with water adsorption. The time constant for water diffusion is calculated and found to be 0.75 hour. The similar time constant value of contact angle decay (Figure 43) for 1mM NaCl indicates the same mechanism of water adsorption with time.

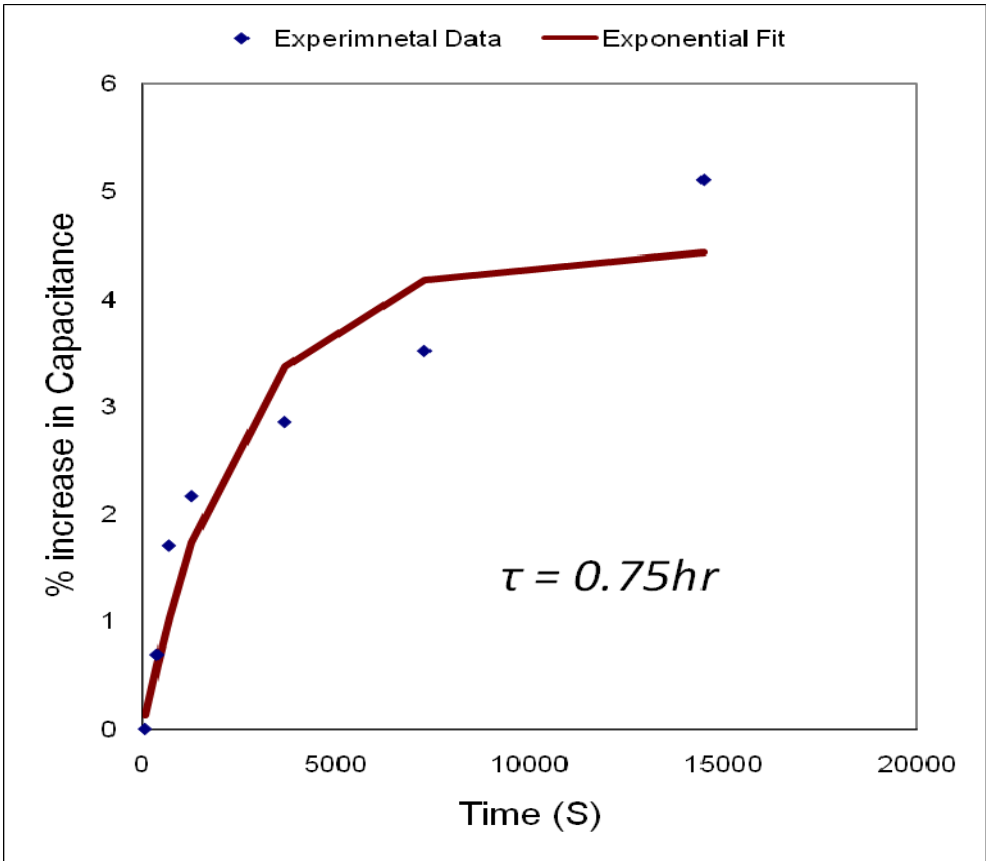

Figure 46 Time Constant of Water Molecule Diffusion in Dielectric Layer

The change in the capacitance with time is believed to be due to the diffusion of water molecules into the CYTOP™ film. The characteristic time (in equation 12) is found by fitting the data to a first order exponential response. From the time constant, the diffusivity constant of electrolyte for each sample is calculated. Based on the capacitance

change, the diffusivity constant of electrolyte in CYTOP™ can be estimated from equation 11. The diffusivity coefficient for the electrolyte were ranged from 1.37 x 10^{-11} cm^2/s to 2.1 x 10^{-12} cm^2/s. Literature report on the diffusivity coefficient for the CYTOP™ film is not available. However, another fluorocarbon polymer of similar nature (Teflon) has been studied before for the diffusion of aqueous NaCl solution [62]. The diffusivity constant is reported to be in the range of 10^{-11} cm^2/s to 10^{-12} cm^2/sec [62].

Also calculations were made for the dielectric constant of the CYTOP™ film and water absorption based on the EIS data obtained. For calculation of dielectric constant actual area of dielectric layer (= 4.9cm^2) was used. These dielectric constant values were calculated after the first set of data are observed (immersion time t= 2min 35sec). The calculate values are listed in Table 2.

Table 2 Dielectric Constant and Water Uptake for Samples

Sample Number	Dielectric Constant Calculated	Water uptake (percentage volume)
1	1.51	0.10
2	1.52	0.11
3	1.53	0.035

The graphical comparison of samples with respect to increase in capacitance with immersion time, dielectric constant calculated and water uptake is shown in Figure 47.

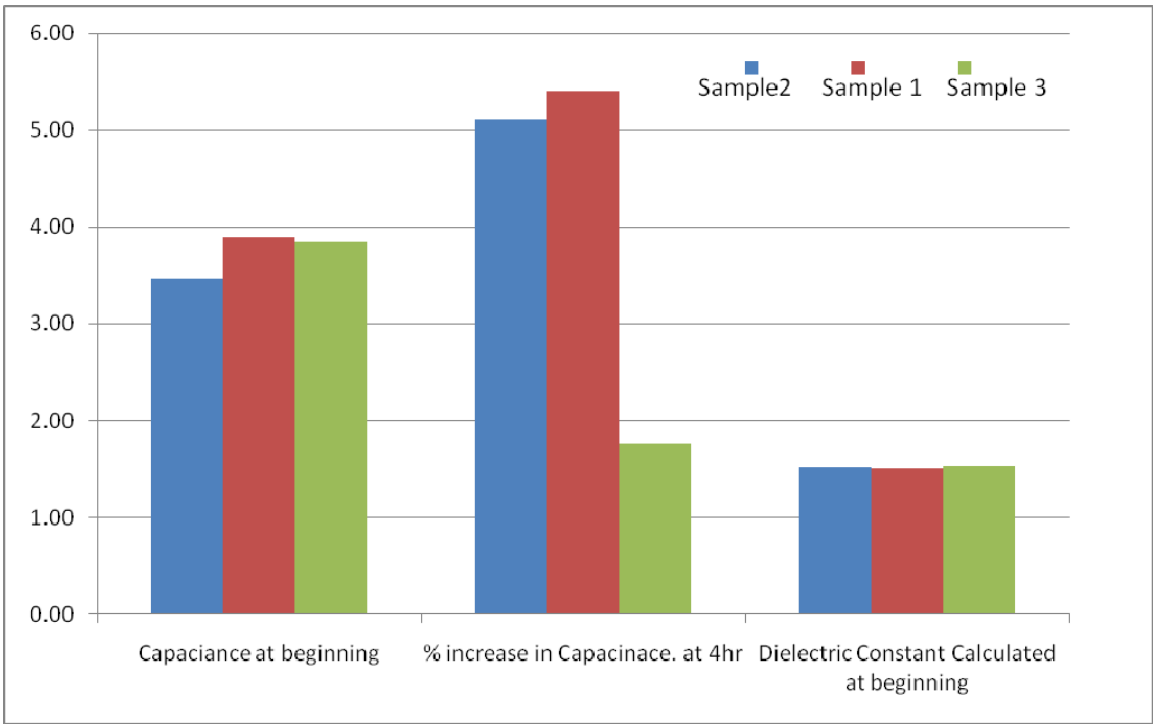

Figure 47 Comparison of Different Samples with Respect to Capacitance after the First Data Collected of the Experiment (t=155 seconds); Percentage Increase in Capacitance at 4hrs and Dielectric Constant Calculated at t=155 seconds.

The capacitance of the CYTOP™ film in contact with 0.1mM NaCl electrolyte was found to increase moderately after 4 hours of immersion. The increase ranged from 1.77% to 5.4% over the initial value. The initial value of the capacitance (~3.5 nF) was approximately consistent with the surface area of the sample (~5 cm^2), the thickness of the coating (~1.8 µm) and the expected value of the dielectric constant (~2.1 based on values reported in the literature [63]).The value of the dielectric constant of CYTOP™ calculated from the EIS data was on average 1.52, nearly the same for all samples (range: 1.51 to 1.53). The calculated percentage water uptake in the CYTOP™ layer for different samples ranged from 0.03% to 0.11% after 4 hours of immersion time. Water adsorption by the organic coating can degrade the electrowetting system performance substantially. More experiments are needed to have insightful knowledge of the corrosion in microfludic devices. These initial EIS tests were conducted successfully and suggest that

impedance measurements can be a powerful technique to investigate the performance of electrowetting actuated microfluidic devices where CYTOP™ films are used as the dielectric layer.

CHAPTER 6 CONCLUSIONS AND FUTURE WORK

6.1 Conclusions

The electrowetting process is proved to be a powerful method for the tuning of surface energy in accordance with electrical energy. The electrowetting system performance depends on the liquid type, voltage, environmental conditions and quality of the dielectric layer. These parameters of interest have been investigated by various experimental techniques.

However, the conventional contact angle measurement technique does not reveal the change in system performance spontaneously. The contact angle measurement has been done for different liquids. The contact angle measurements exhibited the polarity dependence of electrowetting.

The performance of the electrowetting system has been investigated by direct measurement of the electrowetting force. A lumped system model has been developed and the electrowetting force for different dielectric layers and droplets was predicted. The change in capillary force due to electrical energy was directly measured by using a nanoindenter. The EWF measurements have been done for different liquids and the performance has been discussed. At higher voltages, the charge is being trapped in dielectric layer and performance degrades significantly. The degradation in performance at higher voltages is more in salt solution as compared to DI water. The electrowetting

system performance for the case when the dielectric layer is defected was well captured by EWF measurements.

The environmental exposure of the electrowetting system has been investigated by measuring the contact angle over time and electrochemical impedance spectroscopy. The change in the dielectric layer with water adsorption degrades the system performance. The contact angle modulation changes by as high as 45% for continuous liquid exposure period of 24 hours .The change in dielectric constant with liquid immersion has been measured by impedance spectroscopy. The dielectric constant changes due to water absorption in dielectric layer and highest change observed is 5.3% for immersion time of 4 hours. Initial results conclude that the electrochemical impedance spectroscopy can be used to study the electrochemical corrosion in electrowetting system for microfluidic applications.

6.2 Future Work

The various experimental techniques should be extended to investigate the overall optimization of electrowetting system. The future work includes:

- The EWF measurements more AC voltage to investigate the electrowetting system performance. The parameters of interest for experiments will be various rms AC voltages and frequencies.
- The EWF measurements for substrate immersed in liquid solutions. The EWF data will be related to the contact angle and electrochemical impedance spectroscopy measurements for a better understanding of electrochemical corrosion in electrowetting systems.

- The use of different metal electrodes other than aluminum in electrowetting system. The use of noble metal such as gold can potentially reduce the corrosion in electrowetting system.
- The use of different dielectric films other than CYTOP™ in electrowetting process. The Teflon and Parelyne will be used as the dielectric layer and performance of the electrowetting system will be investigated.
- The more detailed experiment using electrochemical impedance spectroscopy to investigate the electrochemical corrosion in electrowetting system.

REFERENCES

[1] Sung, K., 2003, "Creating, Transporting, Cutting, and Merging Liquid Droplets by Electrowetting-Based Actuation for Digital Microfluidic Circuits," Journal of Microelectromechanical Systems, 12(1) pp. 70.

[2] Pollack, M. G., Shenderov, A. D., and Fair, R. B., 2002, "Electrowetting-Based Actuation of Droplets for Integrated Microfluidics," Lab on a Chip, 2(2) pp. 96.

[3] Paik, P., Pamula, V. K., and Fair, R. B., 2003, "Rapid Droplet Mixers for Digital Microfluidic Systems," Lab on a Chip, 3(4) pp. 253.

[4] Fowler, J., Hyejin Moon, and Chang-Jin Kim, 2002, "Enhancement of mixing by droplet-based microfluidics," IEEE, pp. 97.

[5] Mach, P., Krupenkin, T., Yang, S., 2002, "Dynamic Tuning of Optical Waveguides with Electrowetting Pumps and Recirculating Fluid Channels," Applied Physics Letters, 81(2) pp. 202.

[6] Mohseni, K., and Baird, E. S., 2007, "Digitized Heat Transfer using Electrowetting on Dielectric," Nanoscale and Microscale Thermophysical Engineering, 11(1) pp. 99.

[7] Mohseni, K., 2005, "Effective Cooling of Integrated Circuits using Liquid Alloy Electrowetting," pp. 20, IEEE Semiconductor Thermal Measurement and Management Symposium, San Jose CA.

[8] Bahadur, V., and Garimella, S. V., 2008, "Energy Minimization-Based Analysis of Electrowetting for Microelectronics Cooling Applications," Microelectronics Journal, 39(7) pp. 957.

[9] Oprins, H., 2007, "On-Chip Liquid Cooling with Integrated Pump Technology," IEEE Transactions on Components and Packaging Technologies, 30(2) pp. 209.

[10] Matsumoto, H., and Colgate, J.E., 1990, "Preliminary investigation of micropumping based on electrical control of interfacial tension," Proceedings. IEEE Micro Electro Mechanical Systems., Napa Valley, CA, USA, pp. 105.

[11] Mugele, F., Baret, J. C., and Steinhauser, D., 2006, "Microfluidic Mixing through Electrowetting-Induced Droplet Oscillations," Applied Physics Letters, 88(20) pp. 204106.

[12] Chen, J. Y., Kutana, A., Collier, C. P., 2005, "Electrowetting in Carbon Nanotubes," Science, 310(5753) pp. 1480.

[13] Berge, B., and Peseux, J., 2000, "Variable Focal Lens Controlled by an External Voltage: An Application of Electrowetting," The European Physical Journal.E, Soft Matter, 3(2) pp. 159.

[14] Krupenkin, T., Yang, S., and Mach, P., 2003, "Tunable Liquid Microlens," Applied Physics Letters, 82(3) pp. 316.

[15] Kuiper, S., and Hendriks, B. H. W., 2004, "Variable-Focus Liquid Lens for Miniature Cameras," Applied Physics Letters, 85(7) pp. 1128.

[16] Hayes, R. A., and Feenstra, B. J., 2003, "Video-Speed Electronic Paper Based on Electrowetting," Nature, 425(6956) pp. 383.

[17] Heikenfeld, J. C., Smith, N. R., Sun, B., 2008, "Flat Electrowetting Optics and Displays," Proceedings of SPIE--the International Society for Optical Engineering, 6887pp. 688705.

[18] Heikenfeld, J., 2008, "Flat Electrowetting Optics and Displays," Proc. SPIE - Int. Soc. Opt. Eng., pp.6887.

[19] Roques Carmes, , 2004, "Liquid Behavior Inside a Reflective Display Pixel Based on Electrowetting," Journal of Applied Physics, 95(8) pp. 4389.

[20] Beni, G., 1981, "Dynamics of Electrowetting Displays," Journal of Applied Physics, 52(10) pp. 6011.

[21] Cooney, C. G., 2006, "Electrowetting Droplet Microfluidics on a Single Planar Surface," Microfluidics and Nanofluidics, 2(5) pp. 435.

[22] Kuo, J. S., 2003, "Electrowetting-Induced Droplet Movement in an Immiscible Medium," Langmuir, 19(2) pp. 250.

[23] Mugele, F., 2005, "Electrowetting: From Basics to Applications," Journal of Physics. Condensed Matter, 17(28) pp. R705.

[24] Quinn, A., 2005, "Contact Angle Saturation in Electrowetting," Journal of Physical Chemistry B, 109(13) pp. 6268.

[25] Seyrat, E., 2001, "Amorphous Fluoropolymers as Insulators for Reversible Low-Voltage Electrowetting," Journal of Applied Physics, 90(3) pp. 1383.

[26] Verheijen, H. J. J., 1999, "Reversible Electrowetting and Trapping of Charge: Model and Experiments," Langmuir, 15(20) pp. 6616.

[27] Yeo, L. Y., 2006, "Electrowetting Films on Parallel Line Electrodes," Physical Review. E, Statistical, Nonlinear, and Soft Matter Physics, 73(1) pp. 11605.

[28] Yuejun, Z., 2007, "Micro Air Bubble Manipulation by Electrowetting on Dielectric (EWOD): Transporting, Splitting, Merging and Eliminating of Bubbles," Lab on a Chip, 7(2) pp. 273.

[29] Zhiliang, W., 2007, "Reversible Electrowetting of Liquid-Metal Droplet," Journal of Fluids Engineering, 129(4) pp. 388.

[30] Verheijen, H. J. J., 1999, "Contact Angles and Wetting Velocity Measured Electrically," Review of Scientific Instruments, 70(9) pp. 3668.

[31] Schaffer, E., and Po-Zen Wong, 1998, "Dynamics of Contact Line Pinning in Capillary Rise and Fall," Physical Review Letters, 80(14) pp. 3069.

[32] Peykov, V., 2000, "Electrowetting: A Model for Contact-Angle Saturation," Colloid Polymer Science, 278(8) pp. 789.

[33] Baird, E., 2007, "Comparison of Electrowetting on Dielectric and Dielectrophoresis Force Distributions," AIAA Paper, .

[34] Seyrat, E., and Hayes, R. A., 2001, "Amorphous Fluoropolymers as Insulators for Reversible Low-Voltage Electrowetting," Journal of Applied Physics, 90(3) pp. 1383.

[35] Bahadur, V., 2007, "Electrowetting-Based Control of Static Droplet States on Rough Surfaces," Langmuir, 23(9) pp. 4918.

[36] Moon, H., 2002, "Low Voltage Electrowetting-on-Dielectric," Journal of Applied Physics, 92(7) pp. 4080.

[37] Cahill, B. P., Giannitsis, A. T., Land, R., 2008, "Optimization of Electrowetting Electrodes: Analysis of the Leakage Current Characteristics of various Dielectric Layers," pp. 79.

[38] Raj, B., Smith, N. R., Christy, L., 2008, "Composite Dielectrics and Surfactants for Low Voltage Electrowetting Devices," pp. 187.

[39] Banpurkar, A. G., Duits, M. H. G., Van Den Ende, D., 2009, "Electrowetting of Complex Fluids: Perspectives for Rheometry on Chip," Langmuir, 25(2) pp. 1245.

[40] Baviere, R., 2008, "Dynamics of Droplet Transport Induced by Electrowetting Actuation," Microfluidics and Nanofluidics, 4(4) pp. 287.

[41] Walker, S. W., and Shapiro, B., 2006, "Modeling the Fluid Dynamics of Electrowetting on Dielectric (EWOD)," Journal of Microelectromechanical Systems, 15(4) pp. 986-1000.

[42] Berthier, J., Dubois, P., Clementz, P., 2007, "Actuation Potentials and Capillary Forces in Electrowetting Based Microsystems," Sensors and Actuators, A: Physical, 134(2) pp. 471-479.

[43] L.L Shreir , R.A.Jarman , G.T.Burtein, 1998, "Corrosion Volumee 2," Butterworth Heinemann, Oxford, .

[44] Craig R. Barrett, William D.Nix,Alan S.Tetelman, 1973, "The Principles of Engineering Materials," Prentice Hall, New Jersey, .

[45] Sagüés, A. A., Wolan, J. T., Fex, A. D., 2006, "Impedance Behavior of Nanoporous SiC," Electrochimica Acta, pp. 1656.

[46] Adamiak, K., 2006, "Capillary and Electrostatic Limitations to the Contact Angle in Electrowetting-on-Dielectric," Microfluidics and Nanofluidics, 2(6) pp. 471.

[47] Drygiannakis, A., 2009, "On the Connection between Dielectric Breakdown Strength, Trapping of Charge, and Contact Angle Saturation in Electrowetting," Langmuir, 25(1) pp. 147.

[48] Berry, S., 2007, "Irreversible Electrowetting on Thin Fluoropolymer Films," Langmuir, 23(24) pp. 12429.

[49] Shih-Kang, F., 2007, "Asymmetric Electrowetting-Moving Droplets by a Square Wave," Lab on a Chip, 7(10) pp. 1330.

[50] Wang, T., 2006, "Droplets Oscillation and Continuous Pumping by Asymmetric Electrowetting," 2006pp. 174.

[51] Vallet, M., Vallade, M., and Berge, B., 1999, "Limiting Phenomena for the Spreading of Water on Polymer Films by Electrowetting," The European Physical Journal.B, 11(4) pp. 583.

[52] Shea, H. R., Gasparyan, A., Ho Bun Chan, 2004, "Effects of Electrical Leakage Currents on MEMS Reliability and Performance," IEEE Transactions on Device and Materials Reliability, 4(2) pp. 198.

[53] Yang, P., and Chern, J., 1993, "Design for Reliability: The Major Challenge for VLSI," Proceedings of the IEEE, 81(5) pp. 730.

[54] Herrmann, H. J., 1990, "Fracture Patterns and Scaling Laws," Physica A, 163(1) pp. 359.

[55] Frankel, G. S., Russak, M. A., Jahnes, C. V., 1989, "Pitting of Sputtered Aluminum Alloy Thin Films," Journal of the Electrochemical Society, 136(4) pp. 1243.

[56] Nanayakkara, Y., 2008, "A Fundamental Study on Electrowetting by Traditional and Multifunctional Ionic Liquids: Possible use in Electrowetting on Dielectric-Based Microfluidic Applications," Analytical Chemistry, 80(20) pp. 7690.

[57] Lee, S., 2008, "The Wettability of Fluoropolymer Surfaces: Influence of Surface Dipoles," Langmuir, 24(9) pp. 4817.

[58] Wang, X., 2005, "Dynamic Behavior of Polymer Surface and the Time Dependence of Contact Angle," Science in China Series B: Chemistry, 48(6) pp. 553.

[59] Li, G., 2007, "Time-Dependence of Pervaporation Performance for the Separation of ethanol/water Mixtures through Poly(Vinyl Alcohol) Membrane," Journal of Colloid and Interface Science, 306(2) pp. 337.

[60] Carey, D., 2000, "Entropically Influenced Reconstruction at the PBD-ox/water Interface: The Role of Physical Cross-Linking and Rubber Elasticity," Macromolecules, 33(23) pp. 8802.

[61] Berglin, M., 2003, "Fouling-Release Coatings Prepared from Alpha , Omega -Dihydroxypoly(Dimethylsiloxane) Cross-Linked with (Heptadecafluoro-1,1,2,2-Tetrahydrodecyl)Triethoxysilane," Journal of Colloid and Interface Science, 257(2) pp. 383.

[62] A.L lordanski. A.L. Shterezon, Yu. V. Moissev and G.E Zakiov, 1979, "Diffusion of Electrolyte Sin Polymer," Russian Chemical Reviews, 8(48) pp. 781.

[63] http://www.agc.co.jp/english/chemicals/shinsei/cytop/cytop.htm